Protonation and Free Energy Changes Associated with Formation of Q_BH_2 in Native and Glu-L212 → Gln Mutant Reaction Centers from *Rhodobacter sphaeroides*†

P. H. McPherson, M. Schönfeld,‡ M. L. Paddock, M. Y. Okamura, and G. Feher*

Department of Physics, University of California, San Diego, 9500 Gilman Drive, La Jolla, California 92093-0319

Received September 3, 1993; Revised Manuscript Received November 3, 1993®

ABSTRACT: Formation of the quinol Q_BH_2 in Glu-L212 → Gln mutant [EQ(L212)] reaction centers (RCs) from *Rhodobacter sphaeroides* was investigated by measuring the proton uptake (using dyes), UV absorption changes, and free energy changes associated with the two-electron reduction of Q_B. The advantage of using the EQ(L212) RCs for these studies is that the individual protonation steps can be kinetically resolved and analyzed; conclusions reached regarding the mechanism of formation of Q_BH_2 are expected to apply also to native RCs. The proton uptake by EQ(L212) RCs was strongly biphasic: the fast phase was essentially concomitant with the second electron transfer to Q_B^- (~1 ms at pH 7.5); the slow phase was ~2000-fold slower. The rate constant of the slow phase depended on the redox state of the primary quinone Q_A; for Q_A^- the rate constant was larger (i.e., 8-fold at pH 6.0) than for Q_A. The electron and proton transfers to Q_B^- in EQ(L212) RCs were modeled with a two-step scheme as follows: (1) *fast*, $Q_A^-Q_B^- + H^+(1) \rightarrow Q_A(Q_BH)^-$; (2) *slow*, $Q_A(Q_BH)^- + H^+(2) \rightarrow Q_AQ_BH_2$, where reaction 1 involves concomitant electron transfer and proton uptake [Paddock, M. L., McPherson, P. H., Feher, G., & Okamura, M. Y. (1990) *Proc. Natl. Acad. Sci. U.S.A. 87*, 6803–6807]. The stoichiometry of the *fast* proton uptake associated with the two-electron reduction of Q_B varied from 1.1 to 1.4 $H^+/2e^-$ at pH 6.5–8.5, consistent with the uptake of $H^+(1)$ plus an additional fractional proton uptake due to amino acid residues whose pK_a values are shifted by interactions with the charge of $(Q_BH)^-$. The *total steady-state* proton uptake stoichiometry was 2.0 $H^+/2e^-$ at pH ≤ 7.5, consistent with the formation of the quinol Q_BH_2 (reactions 1 and 2). At pH 8.5, the steady-state proton uptake was 1.6 ± 0.1 $H^+/2e^-$, which is consistent with an apparent pK_a for $H^+(2)$ of ~8.5 [McPherson, P. H., Okamura, M. Y., & Feher, G. (1993) *Biochim. Biophys. Acta 1144*, 309–324]. The proton uptake kinetics indicate that Glu-L212 is a component of the proton transfer chain for $H^+(2)$ that connects reduced Q_B (buried in the RC protein) to the aqueous solvent as proposed previously [Paddock, M. L., Rongey, S. H., Feher, G., & Okamura, M. Y. (1989) *Proc. Natl. Acad. Sci. U.S.A. 86*, 6602–6606]. To determine which species protonates slowly in EQ(L212) RCs, i.e., either $(Q_BH)^-$ (as shown in reaction 2) or an internal residue (e.g., His-L190) that rapidly transfers a proton to $(Q_BH)^-$, we measured the UV difference spectrum associated with the slow proton uptake. The difference spectrum resembles that for the protonation of the quinol anion $(QH)^-$ in 80% ETOH, supporting the model shown in reaction 2. This means that the second electron transfer to Q_B^- can occur with only one proton as shown in reaction 1. The free energy changes ΔG_1° and ΔG_2° associated with reactions 1 and 2, respectively, were deduced from the equilibrium partitioning (measured spectroscopically) between $Q_A^-Q_B^-$ and Q_B^{2-}. The free energy ΔG_1° is linear with pH between 8.0 and 9.5 with a slope of 63 ± 3 meV/pH as expected for the uptake of one [i.e., $H^+(1)$] proton. At pH <9.0, $Q_A(Q_BH)^-$ is energetically favored relative to $Q_A^-Q_B^-$, while for pH >9.0 $Q_A^-Q_B^-$ is energetically favored. The free energy ΔG_2° is >0 at pH >9.0 indicating that the pK_a associated with $H^+(2)$ is <9.0, in agreement with the pK_a of ~8.5 observed for the proton uptake. From the free energy changes one can in principle determine whether the activated intermediate state in reaction 1 is the unprotonated state $Q_AQ_B^{2-}$ or the protonated state $Q_A^-(Q_BH)$. An analysis using simplifying assumptions favors $Q_AQ_B^{2-}$ as the intermediate state.

Proton transfer is a crucial part of photosynthesis, i.e., the conversion of light into electrochemical energy. This energy conversion is mediated in bacterial photosynthesis by a protein–pigment complex called the reaction center (RC) that spans the bacterial membrane. The reaction center [reviewed in Parson (1987) and Feher et al. (1989)] consists of three polypeptide subunits, L, M, and H, and nine prosthetic groups: four bacteriochlorophyll molecules, two of which form a dimer that serves as a primary electron donor (D),[1] two bacteriopheophytin molecules, two ubiquinone-50 molecules that serve as primary (Q_A) and secondary (Q_B) electron acceptors, and a non-heme iron Fe^{2+}. The reaction center couples the absorption of light to the uptake of protons through a photocycle involving a series of light-induced electron and

† This work was supported by the National Science Foundation (DMB89-15631) and the National Institute of Health (GM13191; P.H.M. and M.L.P. were partially supported by NIH training grants).

* Address correspondence to this author (Fax: 619 534-0173).

‡ Current address: Faculty of Agriculture, The Hebrew University of Jerusalem, P.O. Box 12, Rehovot 76100, Israel.

® Abstract published in *Advance ACS Abstracts,* January 15, 1994.

[1] Abbreviations: D, primary donor; Q_A, primary acceptor, Q_B, secondary acceptor; $(Q_BH)^-$, quinol (dihydroquinone) anion of secondary acceptor; Q_BH_2 quinol of secondary acceptor; $H^+(1)$, first proton taken up to form $(Q_BH)^-$; $H^+(2)$, second proton taken up to form Q_BH_2; RC, reaction center; cyt *c*, cytochrome *c*; DAD, diaminodurene; Q_{10}, ubiquinone-50; LDAO, lauryldimethylamine *N*-oxide; CMC, critical micelle concentration.

0006-2960/94/0433-1181$04.50/0

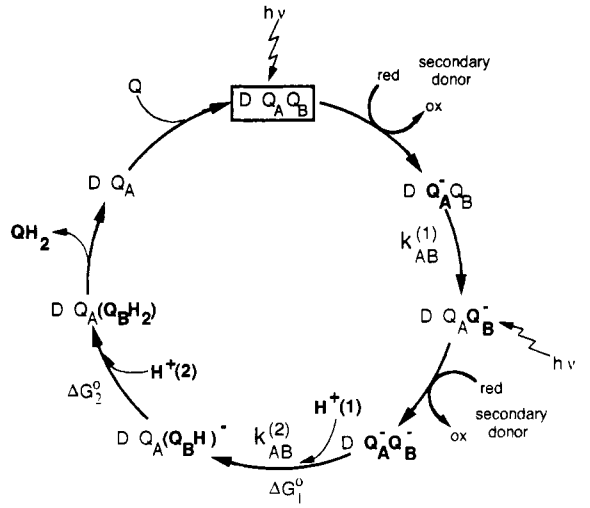

FIGURE 1: RC photocycle. The first step (starting at top) is reduction of the primary quinone Q_A (a Q_{10} molecule) by the following sequential reactions (not all shown): (i) absorption of a photon to form the excited primary donor D* (D is a bacteriochlorophyll dimer), (ii) electron transfer in 3 ps from D* to the intermediate acceptor ϕ_A (a bacteriopheophytin molecule) to form $D^+\phi_A^-$, (iii) electron transfer in ~100 ps from ϕ_A^- to the primary quinone Q_A to form $D^+Q_A^-$, and (iv) reduction of the oxidized primary donor D^+ by cyt c^{2+} in 1–100 μs to form DQ_A^-. Subsequent steps involve electron transfer $k_{AB}^{(1)}$ from Q_A^- to the secondary acceptor quinone Q_B (a Q_{10} molecule) to form $DQ_AQ_B^-$ (in 150 μs at pH 7) followed by a repeat of reactions i–iv to form $DQ_A^-Q_B^-$. Electron transfer $k_{AB}^{(2)}$ (in ~1 ms at pH 7) and the uptake of two protons (from the cytoplasm in bacteria) lead to the formation of the quinol Q_BH_2. The final steps are quinol release (into the membrane *in vivo*) followed by binding of a neutral quinone. In the bacterium, the released quinol is reoxidized by the bc_1 complex, releasing the two protons into the periplasm which leads to the formation of the chemiosmotic proton gradient across the bacterial membrane. Not shown is the fractional ($<1.0\ H^+/e^-$) proton uptake by amino acid residues that interact with Q_A^- and Q_B^-. The overall rate of the photocycle (obtained from the rate of cyt c^{2+} photooxidation) is ~1000 cycles/s at pH 7.5.

proton transfer reactions (see Figure 1) [reviewed in Wraight (1982), Parson (1987), Kirmaier and Holten (1987), Feher et al. (1989), and Okamura and Feher (1992)]. Electron transfer in the RC and the uptake of two protons from the cytoplasm leads to the formation of a loosely bound quinol, Q_BH_2, which is released from the RC into the bacterial membrane and oxidized by the cytochrome bc_1 complex [reviewed in Dutton (1986), and Cramer and Knaff (1990)], releasing the two protons into the periplasm. The gradient of protons thus formed across the bacterial membrane supplies energy for various cellular functions, e.g., synthesis of ATP from ADP [reviewed in Nicholls (1982) and Cramer and Knaff (1990)]. Formation of the quinol Q_BH_2 in the RC is the first step in this process and is the subject of this work.

The secondary quinone Q_B is buried inside the RC protein out of contact with the aqueous solvent (Allen et al., 1988). The uptake of protons to form Q_BH_2 occurs along a series of protonatable groups that connect Q_B to the surface of the RC. Examination of the crystal structure of the RC shows several possible pathways that involve both protonatable amino acid side chains of the RC and bound water molecules (Allen et al., 1988; Beroza et al., 1992). The role of the amino acid side chains has been tested experimentally using site-specific mutagenesis to replace protonatable groups with nonprotonatable ones [reviewed in Okamura and Feher (1992) and Takahashi and Wraight (1993)]. Replacements of Ser-L223 (Paddock et al., 1990), Asp-L213 (Paddock et al., 1990; Takahashi & Wraight, 1990; McPherson et al., 1991; Paddock et al., 1993), and Glu-L212 (Paddock et al., 1989; McPherson et al., 1990; Takahashi & Wraight, 1992) have implicated these residues as components in the proton transfer chains.

In this work we examine the electron and proton transfer reactions in RCs in which the protonatable residue Glu-L212 was replaced with its nonprotonatable analog Gln [EQ(L212) mutant RCs]. In preliminary work by us (Feher et al., 1990; McPherson et al., 1990) and Takahashi and Wraight (1992), the proton uptake by doubly reduced Q_B in EQ(L212) RCs was observed to have a slow phase, consistent with the proposal of Paddock et al. (1989) that the mutation reduces the rate of proton uptake, thereby implicating Glu-L212 as a component of the chain. However, in these studies, neutral quinone that was present in excess had replaced Q_BH_2 in the Q_B pocket (see Figure 1). Recent results obtained on native RCs suggest that protonation of *bound* doubly reduced Q_B is significantly different than that of *free* doubly reduced quinone (McPherson et al., 1993a). Consequently, some of the observed proton uptake could be associated with the quinone/quinol exchange (last two steps in Figure 1), in which case the observed kinetics would be difficult to interpret in terms of the rate of protonation of Q_B^{2-} inside the RC. To investigate this possibility, we measured the proton uptake in the absence of excess neutral quinone.

We measured with dyes the kinetics and stoichiometry of the proton uptake by EQ(L212) RCs at pH 6.5–8.5 in the absence of excess neutral quinone. We discuss the results in terms of the effect of the mutation on the on-rate and off-rate of the proton for bound doubly reduced Q_B. We compare the proton uptake with that predicted by the model for proton and electron transfer that was proposed by Paddock et al. (1990). We also investigated the effect of the redox state of Q_A on the kinetics of the proton uptake.

To determine which group protonates slowly in the mutant, we measured the UV difference spectrum associated with the slow proton uptake by doubly reduced Q_B in the EQ(L212) RCs. These results are discussed in terms of whether or not a fast internal proton transfer to doubly reduced Q_B (e.g., from His-L190) precedes the uptake of the second proton from solution as was proposed by Paddock et al. (1990).

The equilibrium partition coefficient β between the states $Q_A^-Q_B^-$ and $Q_AQ_B^{2-}$ (protonation omitted for simplicity) before and after the slow proton uptake was determined at pH 6.5–10.0. From the values of β the free energy changes associated with the fast and slow phases of the proton uptake were determined. An apparent pK_a associated with the slow proton uptake was determined from the free energy changes and compared with that determined from the stoichiometry of the steady-state proton uptake. The free energies determined in the mutant RCs are expected to apply also to native RCs because the steady-state proton uptake stoichiometries and steady-state partition coefficient β to which they are related are approximately the same in native and mutant RCs.

Preliminary accounts of this work have been published (Feher et al., 1990; McPherson et al., 1990, 1993b).

MATERIALS AND METHODS

Reagents, Buffers, and Dyes. Cytochrome *c* (cyt *c*; horse heart grade VI, Sigma) was reduced (>99%) by hydrogen gas in the presence of platinum black (Aldrich), which was removed by filtration (Schleicher and Schuell uniflo filter, 0.2 μm pore size). The concentration of cyt c^{2+} was determined from the optical absorbance using the extinction coefficient $\epsilon_{\text{cyt } c^{2+}}^{550} = 29.5\ \text{mM}^{-1}\cdot\text{cm}^{-1}$ (Van Gelder & Slater, 1962). The amount of cyt c^{2+} oxidized by RCs was quantified using the difference extinction coefficient $\epsilon_{\text{cyt } c^{2+}}^{550} - \epsilon_{\text{cyt } c^{3+}}^{550} = 21.1 \pm 0.4\ \text{mM}^{-1}\cdot\text{cm}^{-1}$ (Van Gelder & Slater, 1962). Solutions of

ferrocene and diaminodurene (DAD; 2,3,5,6-tetramethyl-*p*-phenylenediamine) were prepared in ethanol prior to use. Ubiquinone-50 (Q_{10}; 2,3-dimethoxy-5-methyl-6-decaisoprenyl-1,4-benzoquinone) (Sigma) was solubilized in 1% (w/v) LDAO (lauryldimethylamine *N*-oxide) (Fluka) at 50 °C and stored at −70 °C. Ferrocyanide [$K_4(CN)_6$] (Mallinckrodt) was prepared in water prior to use. Buffers used were Pipes (1,4-piperazinediethanesulfonic acid) (Calbiochem-Behring), pH 6.0–7.0, Hepes (*N*-2-hydroxyethylpiperazine-*N*′-2-ethanesulfonic acid) (Calbiochem-Behring), pH 7.0–8.0, Tris [2-amino-2-(hydroxymethyl)propane-1,3-diol] (Schwarz/Mann), pH 8.0–9.0, and Ches (cyclohexylaminoethanesulfonic acid) (Calbiochem-Behring), pH 9.0–10.0. The following pH sensitive dyes were used at the indicated wavelengths and pH: chlorophenol red (water soluble, Aldrich), pH 6.5, λ = 575 nm; phenol red (sodium salt, Sigma), pH 7.5, λ = 555 nm; cresol red (sodium salt, Sigma), pH 8.5, λ = 555 nm.

Reaction Centers. Reaction centers were isolated in LDAO from the strains *Rhodobacter sphaeroides R-26.1* ("native RCs") and *Rb. sphaeroides ΔLM* 1(*pRKENGln*) ["EQ(L212) mutant RCs"] as described (Paddock et al., 1988, 1989). The amount of bound Q_B was increased by adding Q_{10} in 1% LDAO (after dilution, the LDAO concentration was 0.1%) followed by dialysis for 48 h at 4 °C against 2 mM Tris-HCl, 10 mM KCl, 0.040% dodecyl β-D-maltoside, and 0.1 mM EDTA, pH 8. After dialysis, the RCs contained 1.9 Q/RC, i.e., 1.0 Q_A, 0.7 Q_B, and 0.2 nonspecifically bound Q [determined by a charge recombination kinetics and cyt c^{2+} photooxidation assay as described (Okamura et al., 1982)]. For some experiments, RCs were depleted of Q_B as described (Okamura et al., 1975). The concentration of active RCs was determined from the amount of cyt c^{2+} oxidized after one laser flash (McPherson et al., 1993a); the RC extinction coefficients at 802 nm determined by this procedure were 318 ± 12 $mM^{-1}\cdot cm^{-1}$ (native RCs) and 333 ± 12 $mM^{-1}\cdot cm^{-1}$ [EQ(L212) mutant RCs].

Optical Absorbance Measurements. Steady-state absorbance spectra were recorded on a Cary 17D spectrophotometer (Varian). Absorbance changes at 340 nm < λ < 870 nm were measured using a single-beam spectrophotometer described by Kleinfeld et al. (1984). Ultraviolet absorbance changes (240 nm < λ < 340 nm) were determined using a single-beam spectrophotometer of local design consisting of a deuterium arc lamp (Bausch and Lomb 33-86-35-01; 50 W), a grating monochromator [Bausch and Lomb 33-86-01; spectral bandwidth, 2 nm; higher order lines ($n > 1$) filtered out with a Corning 7-54 filter], and a photomultiplier tube (PMT; RCA IP28). The current from the PMT was converted to a voltage and filtered with electronics of local design, recorded on a digital oscilloscope (LeCroy 9310M), and transferred to a personal computer for analysis.

Actinic Illumination. Closely spaced laser flashes (e.g., Δt = 10 ms) were from two pulsed-dye lasers (Phase-R DL2100c and DL1000; 0.5-μs flash width, ~0.2 J/flash, λ_o = 590 nm). Light saturation of the RCs was determined to be more than 99% from the bleaching at 865 nm as a function of actinic light intensity. Continuous illumination from a projector (Leitz; 500-W tungsten bulb) was passed through water (3 cm), a Corning c 2-64 glass filter, and an interference filter (Corion BB850; bandwidth, 50 nm).

Curve Fitting. Fits to data were obtained using the program Peakfit (Jandel) on an IBM compatible personal computer.

Determination of the Equilibrium Partition Coefficient β. The partition coefficient β is defined by

$$Q_A^-Q_B^- \overset{\beta}{\rightleftharpoons} Q_AQ_B^{2-} \tag{1a}$$

$$\beta = \frac{[Q_A^-Q_B^-]}{[Q_A^-Q_B^-] + [Q_AQ_B^{2-}]} \tag{1b}$$

where protonation has been omitted for simplicity (unless noted, $Q_AQ_B^{2-}$ represents all the protonation states of doubly reduced Q_B). The value of β was determined from two assays (Kleinfeld et al., 1985). In the first, the concentration of $Q_A^-Q_B^-$ after two flashes was determined from the semiquinone absorbance at 450 nm, where neither neutral nor doubly reduced Q_B absorbs. The value of β was obtained from the absorbance changes ΔA_1^{450} and ΔA_2^{450} after one and two flashes using the relation [derived in Kleinfeld et al. (1985)]

$$\beta = \frac{\epsilon^{450}_{Q_AQ_B^-} + \alpha(\epsilon^{450}_{Q_A^-Q_B} - \epsilon^{450}_{Q_AQ_B^-})}{\epsilon^{450}_{Q_A^-Q_B^-}} \frac{(1-\alpha)(1-\delta)\Delta A_1^{450} + \Delta A_2^{450}}{(1-\alpha)(1-\delta)\Delta A_1^{450}} \tag{2}$$

where the ϵ^{450}'s are the extinction coefficients of the various semiquinone states and were determined in native RCs to be (Kleinfeld et al., 1985) (mM^{-1} cm^{-1})

$$\epsilon^{450}_{Q_A^-Q_B} = 4.9 \pm 0.1 \tag{3a}$$

$$\epsilon^{450}_{Q_AQ_B^-} = 6.1 \pm 0.1 \tag{3b}$$

$$\epsilon^{450}_{Q_A^-Q_B^-} = 9.7 \pm 0.3 \tag{3c}$$

[the same values were used for EQ(L212) mutant RCs]. δ is the fraction of RCs without a bound Q_B and α is the equilibrium partition coefficient between $Q_A^-Q_B$ and $Q_AQ_B^-$ defined as follows:

$$Q_A^-Q_B \overset{\alpha}{\rightleftharpoons} Q_AQ_B^- \tag{4a}$$

$$\alpha = \frac{[Q_A^-Q_B]}{[Q_A^-Q_B] + [Q_AQ_B^-]} \tag{4b}$$

The values of δ and α were determined from a charge recombination kinetics assay (Okamura et al., 1982; Kleinfeld et al., 1984).

In the second assay for the partition coefficient β, the concentration of $Q_A^-Q_B^-$ was determined from the amount of cytochrome *c* oxidized (measured at 550 nm) after a series of three flashes. Since the species $DQ_A^-Q_B^-$ cannot oxidize a cyt c^{2+} after a flash (Q_A can accept only one electron), the amount of cyt c^{2+} oxidized after the third flash is reduced with respect to the first flash by an amount determined by the fraction of $DQ_A^-Q_B^-$ formed after the second flash. Note that this method does not rely on the values of extinction coefficients. From the absorption changes, β can be determined as follows [derived in Kleinfeld et al. (1985)]

$$\beta = \frac{(1-\delta)\Delta A_1^{550} - \Delta A_2^{550}}{(1-\delta)\Delta A_1^{550}} + \frac{\Delta A_2^{550} - \Delta A_3^{550}}{\Delta A_2^{550}} \tag{5}$$

Determination of Proton Uptake. Proton uptake was monitored optically using pH indicator dyes (see *Reagents, Buffers, and Dyes*) which were calibrated with known amounts of HCl [see McPherson et al. (1993a) for details of the method]. The proton uptakes by $DQ_AQ_B^-$ and $DQ_AQ_B^{2-}$ were obtained by correcting the observed proton uptakes after one and two laser flashes, respectively, for the fraction of RCs that formed other states [i.e., DQ_A^-, $DQ_A^-Q_B$, and $DQ_A^-Q_B^-$; see Kleinfeld et al. (1985) or McPherson et al. (1993a)]; the corrected values are given by [derived in

McPherson et al. (1993a)]

$$\Delta H^+_{Q_AQ_B^-} = \frac{\Delta H^{+(1)}_{obs} - [\delta + \alpha(1-\delta)]\Delta H^+_{Q_A^-}}{(1-\alpha)(1-\delta)} \quad (6a)$$

$$\Delta H^+_{Q_B^{2-}} = \{\Delta H^{+(2)}_{obs} - [\delta + \alpha^2(1-\delta)]\Delta H^+_{Q_A^-} - [\alpha(1-\alpha)(1-\delta)]\Delta H^+_{Q_AQ_B^-} - [\beta(1-\alpha)(1-\delta)]\Delta H^+_{Q_A^-Q_B^-}\}/\{(1-\beta)(1-\alpha)(1-\delta)\} \quad (6b)$$

where $\Delta H^{+(1)}_{obs}$ and $\Delta H^{+(2)}_{obs}$ are the total observed proton uptakes(H^+/RC) after the first and second flash, respectively, $\Delta H^+_{Q_A^-}$ and $\Delta H^+_{Q_AQ_B^-}$ are the proton uptakes (H^+/e^-) by DQ_A^- and $DQ_AQ_B^-$, and $\Delta H^+_{Q_A^-Q_B^-}$ and $\Delta H^+_{Q_B^{2-}}$ are the proton uptakes ($H^+/2e^-$) by $DQ_A^-Q_B^-$ and $DQ_AQ_B^{2-}$ (we have assumed the proton uptake is the same for DQ_A^- and $DQ_A^-Q_B$). The terms in square brackets represent the mole fractions of each state. The proton uptake by native RCs has been determined previously for the states DQ_A^-, $DQ_AQ_B^-$, and $DQ_AQ_B^{2-}$ (McPherson et al., 1988, 1993a; Maroti & Wraight, 1988a,b). We have determined the proton uptake associated with all these states in the EQ(L212) RCs (the proton uptake by $DQ_A^-Q_B^-$ was approximated to be the sum of $\Delta H^+_{Q_A^-}$ and $\Delta H^+_{Q_AQ_B^-}$).

RESULTS

Proton Uptake

The states $DQ_AQ_B^-$ and $DQ_AQ_B^{2-}$ (protonation omitted for simplicity) were formed after one and two laser flashes, respectively, with ferrocene and ferrocyanide present to reduce D^+ (Maroti & Wraight, 1988b; McPherson et al., 1993a). The proton uptake was measured optically using pH-sensitive dyes (see Materials and Methods) as shown in Figure 2. A small correction (≤2% of $\Delta H^{+(2)}_{obs}$) for the absorbance change of the RCs determined in a strongly buffered (10 mM Hepes at pH 7.5) sample was subtracted. The absorbance change of the dye was calibrated in terms of H^+/RC (right ordinate in Figure 2) by adding known amounts of HCl. The proton uptake by native RCs (Figure 2a) after the second flash is rapid ($k \simeq 1000\ s^{-1}$) and monophasic (McPherson et al., 1993a). The proton uptake by EQ(L212) RCs (Figure 2b) after the second flash is biphasic with a fast rate of $k \simeq 1000\ s^{-1}$ and a slow rate of $k \simeq 0.5\ s^{-1}$.

(1) Stoichiometry. The stoichiometry of proton uptake by DQ_A^-, $DQ_AQ_B^-$, and $DQ_AQ_B^{2-}$ in EQ(L212) RCs is shown in Table 1 for several pH values in the physiological range. The proton uptake by native RCs [obtained from McPherson et al. (1988, 1993a)] is shown for comparison. The proton uptake by DQ_A^- was determined in Q_B-depleted EQ(L212) RCs (see Materials and Methods) after one flash in the presence of ferrocene and ferrocyanide to reduce D^+ (data not shown). The proton uptake by $DQ_AQ_B^-$ was determined from $\Delta H^{+(1)}_{obs}$ (Figure 2b) using eq 6a. The fraction δ of RCs without a bound Q_B and the partition coefficient α were determined from a charge recombination kinetics assay (Okamura et al., 1982; Kleinfeld et al., 1984); at pH 6.5–8.5 δ was 0.32 ± 0.02 and α varied from 0.12 ± 0.03 to 0.18 ± 0.03. The stoichiometry of the fast proton uptake by $DQ_AQ_B^{2-}$ was determined from $\Delta H^{+(2)}_{obs}$ (trans) (see Figure 2b) using eq 6b. The transient values of the partition coefficient β (discussed in a later section; see Figure 7b) were used in eq 6b. The proton uptake by $DQ_A^-Q_B^-$ was approximated to be the sum of the proton uptakes by DQ_A^- and $DQ_AQ_B^-$. The steady-state proton uptake by $DQ_AQ_B^{2-}$ at pH 6.5 and 7.5 was obtained from $\Delta H^{+(2)}_{obs}$ (steady state) (see Figure 2b) and eq 6b (using the steady-state value of β shown in Figure 7b). At pH 8.5, this method was not used because it was too inaccurate due to a slow decay that interfered with the measurement of the slow phase.[2] Therefore, steady-state proton uptake by Q_B^{2-} was determined under continuous illumination, which prevented the decay, with ferrocene and

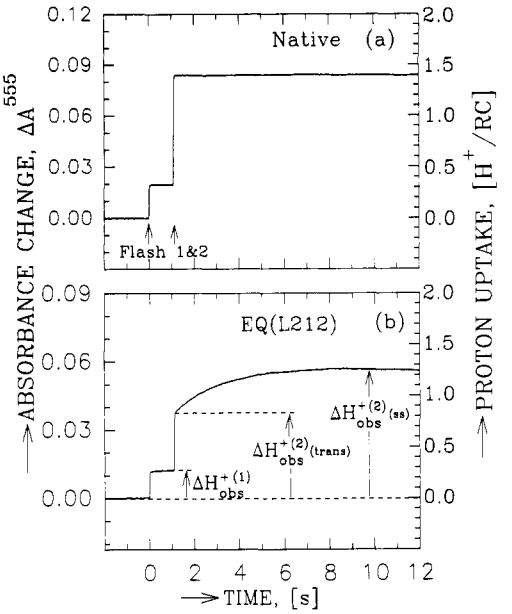

FIGURE 2: Observed proton uptake by native (a) and EQ(L212) mutant (b) RCs determined from the absorbance change of phenol red at 555 nm in the absence of excess quinone. Formation of doubly reduced Q_B occurred ~1 ms after the second flash in a majority of the RCs. The absorbance change was calibrated in terms of H^+/RC (right ordinate) by adding known amounts of HCl. A small (≤2% of $\Delta H^{+(2)}_{obs}$) background absorbance due to RCs determined in a strongly buffered (10 mM Hepes) sample was subtracted. The RC concentration was determined from the amount of cyt c^{2+} oxidized after a single laser flash using the cytochrome c difference extinction coefficient $\epsilon^{550}_{cyt\ c^{2+}} - \epsilon^{550}_{cyt\ c^{3+}} = 21.1\ mM^{-1}\cdot cm^{-1}$. Excess unbound quinone was minimized (~0.2 Q/RC) to prevent replacement of Q_BH_2 in the Q_B pocket with neutral quinone. The proton uptakes by $DQ_AQ_B^-$ and $DQ_AQ_B^{2-}$ (see Table 1) were determined from the observed values $\Delta H^{+(1)}_{obs}$ and $\Delta H^{+(2)}_{obs}$. A small linear decay due to reoxidation of the reduced quinones was subtracted. Conditions: 2 μM RCs, 60 μM ferrocene, 1 mM ferrocyanide, 50 μM phenol red, 0.040% (w/v) dodecyl β-D-maltoside, 50 mM KCl, pH 7.5, 21.5 °C.

Table 1: Stoichiometry of Proton Uptake by Native and EQ(L212) RCs[a]

		proton uptake[b]			
				$\Delta H^+_{Q_B^{2-}}$	
pH	RCs	$\Delta H^+_{Q_A^-}$	$\Delta H^+_{Q_AQ_B^-}$	fast phase[c]	steady state
6.5	native	0.31	0.60	2.02	2.02
	EQ (L212)	0.22	0.67	1.39	2.04
7.5	native	0.31	0.34	1.94	1.94
	EQ (L212)	0.15	0.36	1.31	2.06
8.5	native	0.38	0.44	1.54	1.54
	EQ (L212)	0.05	0.18	1.07	1.56

[a] Proton uptake by native RCs was obtained from McPherson et al. (1988, 1993a) except for steady-state $\Delta H^+_{Q_B^{2-}}$ at pH 8.5 which was determined as discussed in the text. [b] Proton uptakes by DQ_A^- and ($\Delta H^+_{Q_A^-}$) and $DQ_AQ_B^-$($\Delta H^+_{Q_AQ_B^-}$) are due to residues that interact with Q_A^- and Q_B^- are calibrated in terms of H^+/e^- (experimental uncertainty is ±15%). Proton uptake by $DQ_AQ_B^{2-}$($\Delta H^+_{Q_B^{2-}}$) is calibrated in terms of $H^+/2e^-$ (experimental uncertainty is ±6%). [c] Includes proton uptake after the first flash and fast phase of proton uptake after the second flash.

[2] This decay was probably due to oxidation of reduced quinone by ferricyanide.

ferrocyanide as secondary donor to D^+. Under these conditions the state $DQ_A^-Q_B^{2-}$ is formed in the fraction (~0.7) of RCs containing a bound Q_B. The steady-state proton uptake by Q_B^{2-} was obtained by subtracting the small proton uptake by Q_A^- and dividing by the mole fraction of Q_B^{2-}. This mole fraction was determined from the amount of cytochrome *c* oxidized under continuous illumination (Okamura et al., 1982) using the cytochrome *c* extinction coefficient $\epsilon^{550}_{cyt\ c^{2+}} - \epsilon^{550}_{cyt\ c^{3+}} = 21.1 \pm 0.4\ mM^{-1}\cdot cm^{-1}$ (Van Gelder & Slater, 1962). The proton uptake by Q_B^{2-} in native RCs at pH 8.5 obtained with continuous illumination (see Table 1) is in good agreement with that obtained using laser flashes (McPherson et al., 1993a). The two methods of illumination also gave the same result for the fast phase of the proton uptake by the EQ(L212) mutant RCs at pH 8.5.

The steady-state proton uptake by $DQ_AQ_B^{2-}$ in the EQ(L212) and native RCs is the same within experimental error. The proton uptake at pH ≤7.5 is consistent with the uptake of two protons to form the quinol Q_BH_2. At pH 8.5, the proton uptake is significantly smaller than $2.0H^+/2e^-$ (see Discussion).

The stoichiometry of the fast proton uptake by $DQ_AQ_B^{2-}$ in the EQ(L212) RCs is significantly less than the steady-state value but is larger than $1.0H^+/2e^-$. The results are consistent, therefore, with the fast uptake of only one of the protons required to form Q_BH_2. The reason for the fractional proton uptake in excess of $1.0H^+/2e^-$ is given in Discussion.

The proton uptake by $DQ_AQ_B^-$ in the EQ(L212) RCs is similar to that of native RCs at pH 6.5 and 7.5 but is significantly smaller at pH 8.5. The proton uptake by DQ_A^- in the EQ(L212) RCs is smaller than in native RCs, particularly at pH 8.5. The proton uptakes by DQ_A^- and $DQ_AQ_B^-$ are due to amino acid residues whose pK_a values are shifted because of their interaction with Q_A^- and Q_B^- (Wraight, 1979; McPherson et al., 1988; Maroti & Wraight, 1988a,b).

(*2*) *Kinetics.* The rate of the fast phase of proton uptake by $DQ_AQ_B^{2-}$ in EQ(L212) RCs was determined at pH 7.5 from the absorbance change of phenol red (data not shown) as discussed for native RCs in McPherson et al. (1993a). The observed rate was 1200 s^{-1}, which is within 10% the same as that measured in native RCs (McPherson et al., 1993a).

The rate of the slow proton uptake by EQ(L212) RCs was affected by the redox state of Q_A. The absorbance changes of the phenol red after formation of $DQ_AQ_B^{2-}$ and $DQ_A^-Q_B^{2-}$ at pH 7.5 are plotted semilogarithmically in Figure 3. The state $DQ_A^-Q_B^{2-}$ was formed by a third laser flash that occurred 20 ms after the second. A small (~20% of the total amplitude) slow phase due to proton uptake by $DQ_AQ_B^{2-}$ was subtracted from the trace for $DQ_A^-Q_B^{2-}$ (lower curve in Figure 3). This was necessary because $DQ_AQ_B^{2-}$ was formed after three flashes in about 20% of the RCs due to the equilibria shown in eqs 1 and 4. The rates obtained from straight-line fits to the semilog plots in Figure 3 are 0.4 s^{-1} for $DQ_AQ_B^{2-}$ and 2.1 s^{-1} for $DQ_A^-Q_B^{2-}$. Thus, the reduction of Q_A to Q_A^- increases the rate of the slow proton uptake by Q_B^{2-} by a factor of 5 at pH 7.5.

The rate of the slow proton uptake by Q_B^{2-} in the EQ(L212) mutant is only slightly pH dependent (data not shown). The proton uptakes by $DQ_AQ_B^{2-}$ and $DQ_A^-Q_B^{2-}$ slowed down by a factor of ~2 and ~3 per pH unit, respectively, between pH 6.0 and 8.0. The maximum difference between the rates for $DQ_AQ_B^{2-}$ and $DQ_A^-Q_B^{2-}$ was a factor of 8.0 at pH 6.0.

UV Difference Spectrum Associated with the Slow Proton Uptake

The slow proton uptake by EQ(L212) mutant RCs could be due to protonation of either $(Q_BH)^-$ or an amino acid residue that had rapidly protonated $(Q_BH)^-$ (see eq 9 in Discussion). To attempt to discriminate between these two possibilities, we measured the UV difference spectrum associated with the slow proton uptake. The state $DQ_AQ_B^{2-}$ was formed (within ~1 ms) after two laser flashes in the presence of ferrocene to reduce D^+. The UV absorbance changes were measured as shown in Figure 4 (λ = 240 nm). The absolute absorbance change after the second flash had contributions from several RC states and oxidized ferrocene and was, therefore, difficult to interpret. Consequently, we focused on the amplitude ΔA_{trans} of the slow decay ($\tau_{1/e}$ = ~1 s; see Figure 4b) that is associated with the slow proton uptake by the EQ(L212) RCs. The low value of pH (6.5) was chosen to ensure the absence (confirmed at 450 nm) of a slow component of electron transfer which occurs at higher pH (see next section) and would interfere with the measurement. The spectrum was obtained without excess neutral quinone present to minimize any contributions from quinone/quinol exchange (see below).

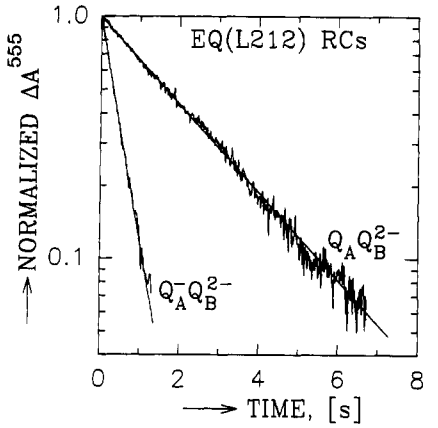

FIGURE 3: Semilog plots of the slow phase of proton uptake (absorbance change of phenol red at 555 nm) by $DQ_AQ_B^{2-}$ and $DQ_A^-Q_B^{2-}$ in EQ(L212) RCs. The states $DQ_AQ_B^{2-}$ and $DQ_A^-Q_B^{2-}$ were formed after two and three flashes, respectively, in the presence of cyt c^{2+} to reduce D^+ (time between flashes: 2nd–1st, 1 s; 3rd–2nd, 20 ms). A small (~20%) slow phase (due to $DQ_AQ_B^{2-}$) was subtracted from the lower trace as discussed in the text. The proton uptake by Q_B^{2-} is 5-fold faster with Q_A reduced (lower trace) than with Q_A oxidized (upper trace). Conditions: 2 μM EQ(L212) RCs, 60 μM cyt c^{2+}, 50 μM phenol red, 0.040% (w/v) dodecyl β-D-maltoside, 50 mM KCl, pH 7.5, 21.5 °C.

The UV difference spectrum associated with the slow proton uptake by the EQ(L212) RCs is shown in Figure 5. The difference extinction coefficient ($\Delta\epsilon_{trans}$) was determined from ΔA_{trans} (see e.g., Figure 4b) using the relation

$$\Delta\epsilon_{trans} = \frac{\Delta A_{trans}}{[RC](1-\delta)(1-\alpha)} \qquad (7)$$

The denominator in eq 7 is the concentration of RCs that form doubly reduced Q_B (the partition coefficient β was omitted from the denominator since it is essentially zero at pH 6.5). The RC concentration ([RC]) was determined as discussed under Materials and Methods, and the fraction δ of RCs without a bound Q_B and the partition coefficient α (see eq 4) were determined as discussed in the proton uptake section. The solid line in Figure 5 is the difference between the extinction coefficients of the UQ_{10} states QH_2 and $(QH)^-$ in 80% ETOH (Morrison et al., 1982). This model spectrum resembles that observed in the EQ(L212) RCs, suggesting that the slow protonation step corresponds to the reaction $(Q_BH)^- + H^+ \rightarrow Q_BH_2$.

As mentioned above, the amount of nonspecifically bound quinone was minimized to prevent exchange of quinol with quinone. This was necessary because the absorbance of quinone may be different in the RC than in solution and,

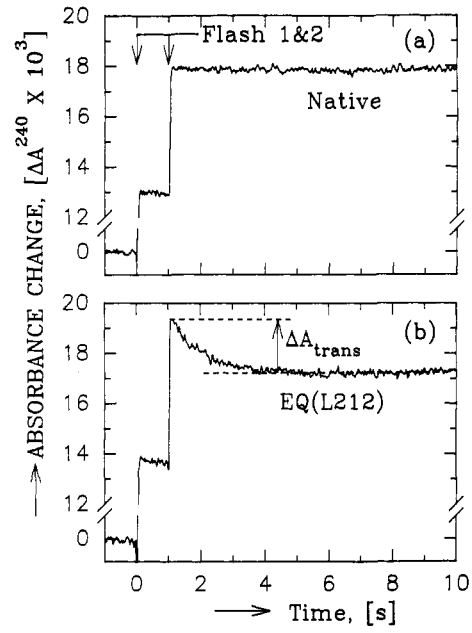

FIGURE 4: UV absorbance changes associated with the formation of Q_BH_2 in native (a) and EQ(L212) (b) RCs. The steady-state absorbances after one and two flashes have contributions from several RC states (see Materials and Methods) and oxidized ferrocene (used to reduce D^+). The slow ($\tau_{1/e} \simeq 1$ s) decay of the absorbance after the second flash in panel b is due to the slow proton uptake (see Figures 2 and 3) by EQ(L212) RCs [essentially all of the electron transfer $k_{AB}^{(2)}$ occurred rapidly ($k > 1000$ s^{-1}) as confirmed at 450 nm]. The difference spectrum shown in Figure 5 was determined from the values of ΔA_{trans} observed at various wavelengths. A slow linear decay due to reoxidation of reduced quinone by oxidized ferrocene was subtracted in panels a and b. Excess unbound quinone was minimized (0.14 Q/RC) to prevent replacement of Q_BH_2 with neutral quinone in the Q_B pocket. Conditions: 1.2 μM RCs, 20 μM ferrocene, 0.040% (w/v) dodecyl β-D-maltoside, 50 mM KCl, 10 mM Pipes, pH 6.5, 21.5 °C.

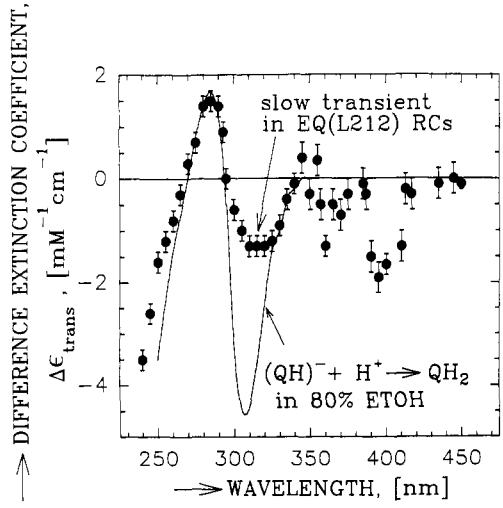

FIGURE 5: UV difference spectrum associated with slow proton uptake in EQ(L212) mutant RCs. The values of $\Delta\epsilon_{trans}$ (filled circles) were determined from the amplitudes ΔA_{trans} of the slow decay after the second flash (see, e.g., Figure 4b) using eq 7. The solid line is the difference between the extinction coefficients of the neutral quinol, QH_2, and the anion quinol $(QH)^-$, in 80% ETOH obtained from Morrison et al. (1982). Conditions: same as given in the legend to Figure 4.

consequently, the quinone/quinol exchange might produce a UV absorbance change that would interfere with the protonation measurements. However, due to the relatively weak binding of Q_B it is impossible to eliminate all the exogenous quinone (Okamura et al., 1982); the EQ(L212) RCs contained about 0.15 Q/RC that were nonspecifically bound and could, in principle, exchange with Q_BH_2 (the extent of this exchange could not be quantified because the binding constants of Q_BH_2 and Q_B are not known). To determine the maximum possible effect of nonspecifically bound quinone, the UV spectrum was remeasured in the presence of excess neutral quinone (~10 Q/RC), which displaced all the doubly reduced Q_B. The spectrum thus obtained (not shown) was significantly different at 260 nm < λ < 310 nm from the one shown in Figure 5, i.e., the maximum value of $\Delta\epsilon_{trans}$ (at 290 nm) was ~4 mM^{-1}·cm^{-1} as compared to ~1.5 mM^{-1}·cm^{-1} in the absence of added quinone. The *maximum possible* effect of quinone/quinol exchange on the spectrum in Figure 5 was estimated by assuming that all of the extra 0.15 Q/RC exchanged with a Q_BH_2 and by using the spectrum with 10 extra Q/RC to extrapolate to the limit of zero quinone/quinol exchange. The corrected spectrum thus obtained was only slightly different than that in Figure 5: the maximum at 285 nm was shifted to 280 nm with essentially no change in amplitude.

Equilibrium Partition Coefficient β

The equilibrium partition coefficient β (defined in eq 1) between the states $Q_A^-Q_B^-$ and $Q_AQ_B^{2-}$ (protonation omitted for simplicity) provides information about the protonation of doubly reduced Q_B (Kleinfeld et al., 1985). Of the two assays used to determine β (see eqs 2 and 5), the semiquinone absorbance assay (eq 2) provides the most information and will, therefore, be discussed in detail.

The absorbance changes at 450 nm of native RCs are shown at pH 7.5 and 9.0 in Figure 6, panels a and b; the lower trace in Figure 6b shows the effect of excess neutral quinone. At 450 nm the semiquinones Q_A^- and Q_B^- absorb but neutral and doubly reduced quinone and DAD (the secondary donor to D^+) do not. The steady-state absorbance increased after the first flash due to formation of semiquinone and decreased after the second flash due to formation of doubly reduced Q_B. A transient absorbance increase after the second flash (unresolved in Figure 6a,b) due to formation of $Q_A^-Q_B^-$ decayed at a rate $k_{AB}^{(2)} \simeq 1500$ s^{-1} (pH 7.5) corresponding to the electron transfer $Q_A^-Q_B^- \rightarrow Q_AQ_B^{2-}$ (Kleinfeld et al., 1985). At pH 7.5 (see Figure 6a), the steady-state concentration of $Q_A^-Q_B^-$ (i.e., β) is essentially zero (quantified below); consequently, the steady-state absorbance after two flashes is due mainly to Q_A^- and Q_B^- which are present as a result of the equilibrium α between $Q_A^-Q_B$ and $Q_AQ_B^-$ (see eq 4) and the fraction δ of RCs without a bound Q_B. At pH 9.0 (upper trace, Figure 6b), the concentration of $Q_A^-Q_B^-$ (i.e., β) is larger than at pH 7.5 causing a larger steady-state absorbance after two flashes. Excess neutral quinone (lower trace, Figure 6b) exchanges with Q_BH_2 driving the protonation steps of the photocycle [$H^+(1)$ and $H^+(2)$; see Figure 1] to completion thereby reducing the concentration of $Q_A^-Q_B^-$ to ~zero.[3]

The absorbance changes of EQ(L212) RCs at 450 nm are shown in Figure 6 panels c and d for pH 7.5 and 9.0; the lower trace in Figure 6d shows the effect of excess neutral quinone. The rate of the fast decay (not resolved in Figure 6c,d) after

[3] The concentration of dodecyl β-D-maltoside for the lower trace of Figure 6b was reduced below the CMC (i.e., to 0.0040% w/v) to obtain 100% fast decay of the absorbance after the second flash. At a concentration above the CMC (0.04% w/v), about 30% of the decay was slow ($\tau_{1/e} \simeq 2$ s; data not shown) corresponding, presumably, to the slow exchange of Q_BH_2 with neutral quinone trapped in detergent micelles. For the lower trace in Figure 6d, the slow kinetics result from the slow proton uptake (see text); the trace was identical for either 0.040% or 0.0040% (w/v) dodecyl β-D-maltoside, because in this case the rate-limiting proton uptake was slower than the exchange of Q_BH_2 with neutral quinone in micelles.

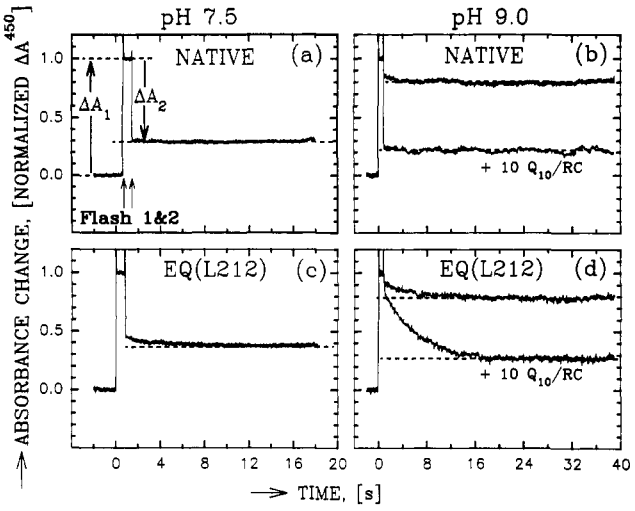

FIGURE 6: Semiquinone absorbance changes at 450 nm in the absence of exogenous quinone (except as noted) from which the partition coefficient β between $Q_A^-Q_B^-$ and $Q_AQ_B^{2-}$ was determined. (a and b) Semiquinone absorbance in native RCs at pH 7.5 and 9.0. At pH 7.5 (a), the steady-state concentration of $Q_A^-Q_B^-$ (β) given by $\Delta A_1^{450} + \Delta A_2^{450}$ is essentially zero; the steady-state absorbance after the second flash is due to the small fraction of RCs containing Q_A^- or Q_B^- (given by α and δ; see eq 4 and associated text). The steady-state absorbance $\Delta A_1^{450} + \Delta A_2^{450}$ is larger at pH 9.0 (upper trace in panel b) than at 7.5 (a) because $[Q_A^-Q_B^-]$ (β) is larger. The lower trace in panel b shows effect of excess neutral quinone, whose exchange with Q_BH_2 (see Figure 1) drives the reaction $Q_A^-Q_B^- + 2H^+ \rightarrow Q_AQ_BH_2$ essentially to completion reducing the observed value of β to zero. The values of β (Figure 7a) were determined from ΔA_1^{450} and ΔA_2^{450} (without excess quinone) using eqs 2 and 3. (c and d) Semiquinone absorbance at 450 nm in EQ(L212) RCs at pH 7.5 and 9.0. The decay of $Q_A^-Q_B^-$ in the presence of excess neutral quinone (lower trace in d) is slow because the exchange of Q with Q_BH_2 occurs after the slow proton uptake. The small absorbance decay after the second flash in the absence of 10 Q/RC is due to decay of $Q_A^-Q_B^-$ caused by (i) the slow proton uptake (see Figure 2) and (ii) exchange of Q_BH_2 with part of the fraction (0.2 Q/RC) of unbound neutral quinone (see Materials and Methods); both i and ii partially drive the equilibrium between $Q_A^-Q_B^-$ and doubly reduced Q_B to completion. A small linear decay due to reoxidation of reduced quinone by oxidized DAD was subtracted from all traces. Conditions: 2 μM RCs, 500 μM DAD, 0.040% dodecyl β-D-maltoside (0.004% for lower traces in b and d), 10 mM pH buffer (see Materials and Methods), 50 mM KCl, 21.5 °C.

the second flash corresponding to electron transfer $Q_A^-Q_B^- \rightarrow Q_AQ_B^{2-}$ was $k_{AB}^{(2)} \simeq 1000\ s^{-1}$ (pH 7.5). This value is approximately the same as in native RCs (Paddock et al., 1989; Takahashi & Wraight, 1992). The small slow decay after the second flash (see Figure 6c and the upper trace in Figure 6d) is associated with the slow proton uptake (see Figure 2b), which shifts the equilibrium between $Q_A^-Q_B^-$ and $Q_AQ_B^{2-}$ toward $Q_AQ_B^{2-}$ (Takahashi & Wraight, 1992). Some of the slow decay probably also results from the exchange of Q_BH_2 with unbound neutral quinone (0.2 Q/RC; see Materials and Methods). The small amplitude of the slow decay shows that the slow proton uptake has only a minor effect on the equilibrium between $Q_A^-Q_B^-$ and doubly reduced Q_B (quantified below). Excess quinone (see the lower trace in Figure 6d) was added to check whether steady state was reached in the EQ(L212) RCs during the monitored period after the second flash. The excess quinone exchanges with Q_BH_2 (see Figure 1), thereby driving the concentration of $Q_A^-Q_B^-$ (β) at *steady state* to zero. The decay of $Q_A^-Q_B^-$ in the EQ(L212) RCs is slow (Figure 6d) because the exchange occurs after the slow proton uptake. At pH $\leq$9.5, the absorbance reached a steady-state value corresponding within experimental error ($\pm$0.07) to $\beta = 0.0$ with a characteristic time constant that varied from 2 s (pH 7.5) to 15 s (pH 9.5).

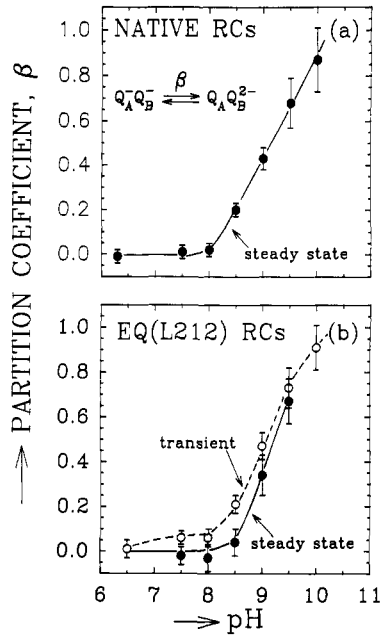

FIGURE 7: Equilibrium partition coefficient β in (a) native RCs and (b) EQ(L212) mutant RCs determined from an average of the semiquinone assay (Figure 6) and the cytochrome *c* photooxidation assay (see text). The transient values of β in the EQ(L212) RCs refer to the equilibrium established between $Q_A^-Q_B^-$ and doubly reduced Q_B during the time period between the fast and slow proton uptakes (see Figure 2). For the model shown in Figure 1, the transient β corresponds to the equilibrium partitioning between $Q_A^-Q_B^-$ and $Q_A(Q_BH)^-$. In native RCs, the uptake of the two protons is not kinetically resolved; consequently, only a steady-state value of β was determined. The steady-state values should be considered to be lower limits, since in a small fraction (<0.2) of RCs unbound neutral quinone may have exchanged with Q_BH_2, which would drive the equilibrium between $Q_A^-Q_B^-$ and doubly reduced Q_B to completion. Error bars are the larger of either (i) errors estimated from the uncertainties in the parameters in eqs 2, 3, and 5 (pH <9.0) or (ii) half the difference between the value of β determined from the two assays (eqs 2 and 5; pH $\geq$9.0). Conditions: same as given in the legend to Figure 6, except 35 μM cyt c^{2+} was used in place of DAD in the cytochrome *c* photooxidation assay.

At pH >9.5 the decay was too slow to measure because of the comparable fluctuations of the baseline; consequently, determination of the steady-state value of β was limited to pH $\leq$9.5 in the EQ(L212) RCs.

The pH dependence of the partition coefficient β in native RCs is shown in Figure 7a. At pH $\geq$7.5 β was determined from an average of the semiquinone assay (see, e.g., Figure 6a,b) using eqs 2 and 3 and the cyt c^{2+} photooxidation assay (data not shown) using eq 5. The values of α and δ were determined using a charge recombination kinetics assay (Okamura et al., 1982; Kleinfeld et al., 1984); their values between pH 6.5 and 10.0 were as follows: α = 0.08–0.22 ($\pm$0.02) and δ = 0.21–0.30 ($\pm$0.02). At pH <7.5 only the cytochrome photooxidation assay was used because the secondary electron donor, DAD, used in the semiquinone assay absorbed and interfered with the measurement. At 7.5 $\leq$ pH $\leq$ 8.5 the results of the semiquinone absorbance and cyt c^{2+} photooxidation assays agreed within experimental error ($\Delta\beta$ = $\pm$0.03). At pH $\geq$9.0, the semiquinone absorbance assay yielded a larger value of β than the cytochrome *c* photooxidation assay; the error bars at pH $\geq$9.0 (Figure 7a) represent half the difference between the two. The pH profile of β is in qualitative agreement with that determined by Kleinfeld et al. (1985) for a different detergent (LDAO) and ionic strength (15 mM).

The pH dependence of β in EQ(L212) mutant RCs is shown in Figure 7b. The values of β were determined as discussed

above for native RCs. The partition coefficient α used in eqs 2 and 5 varied from 0.12 to 0.19 (±0.02) between pH 6.5 and 10.0, and the fraction δ was 0.32 ± 0.02. Two sets of values of β were determined: (*i*) *The transient values* β_{trans}, which correspond to the equilibrium between $Q_A^-Q_B^-$ and $Q_AQ_B^{2-}$ at time (t) $1/k_{fast} \ll t \ll 1/k_{slow}$, where k_{fast} and k_{slow} are the rates of the fast and slow decays at 450 nm after the second flash (at pH 7.5, $1/k_{fast} \simeq 1$ ms and $1/k_{slow} \simeq 0.5$ s). These transient values give the fraction of $Q_A^-Q_B^-$ after the fast electron transfer and proton uptake but before the slow proton uptake. (*ii*) *The steady-state values* β_{ss}, which correspond to the equilibrium between $Q_A^-Q_B^-$ and $Q_AQ_B^{2-}$ at a time $t \gg 1/k_{slow}$, i.e., after the slow proton uptake.

The pH profiles of β in native and EQ(L212) mutant RCs are similar. In both, doubly reduced Q_B is energetically favored over $Q_A^-Q_B^-$ at pH <9. Furthermore, the steady-state value of β in the EQ(L212) mutant RCs is only slightly smaller than the transient value. The small difference between the transient and steady-state values shows that the slow proton uptake has only a minor effect on the extent of electron transfer from $Q_A^-Q_B^-$ to $Q_AQ_B^{2-}$. This is quantified in terms of a free energy change in the next section.

DISCUSSION

We have determined the proton uptake, UV difference spectrum, and free energy changes associated with the formation of Q_BH_2 in RCs in which Glu-L212 was replaced by site-specific mutagenesis (Paddock et al., 1989) with its nonprotonatable analog Gln [EQ(L212)RCs]. The goal of these experiments was two-fold: (i) to understand the role of Glu-L212 in proton uptake by doubly reduced Q_B and (ii) to determine the energetics of proton uptake and the effect of proton uptake on the transfer of the second electron to Q_B^-. The advantage of using the EQ(L212) RCs for these studies is that the individual protonation steps [uptake of $H^+(1)$ and $H^+(2)$; see Figure 1] can be kinetically resolved and analyzed, in contrast to the situation in native RCs. Since the steady-state stoichiometry of proton uptake (see below) and the kinetics of electron transfer are not affected by the mutation, the conclusions regarding protonation and electron transfer in the EQ(L212) RCs are expected to apply also to native RCs.

Glu-L212 is in the vicinity of Q_B, i.e., the carboxyl oxygen of Glu-L212 is ~5 Å from the carbonyl oxygen of Q_B (where protonation occurs) that is hydrogen bonded to His-L190. Previous work by Paddock et al. (1989) showed that mutation of Glu-L212 to Gln significantly slowed the overall rate of the RC photocycle without affecting the rates of the electron transfers $k_{AB}^{(1)}$ and $k_{AB}^{(2)}$ (see Figure 1). This effect was attributed to a slowed proton uptake and led to a model in which Glu-L212 is involved in the proton uptake by reduced Q_B (Paddock et al., 1989). The measurement of proton uptake with dyes is the most direct test of this model and is discussed first.

Proton Uptake by Doubly Reduced Q_B. The mutation Glu-L212 → Gln significantly changes the *kinetics* of proton uptake by doubly reduced Q_B (see Figure 2) without affecting the *steady-state stoichiometry* (see Table 1). In native RCs, the proton uptake by doubly reduced Q_B occurs essentially concomitant with electron transfer $k_{AB}^{(2)}$ from $Q_A^-Q_B^-$ to Q_B^{2-} in ~1 ms at pH 7.5 (McPherson et al., 1993a). In EQ(L212) RCs, the proton uptake is biphasic: the fast phase is essentially concomitant with electron transfer $k_{AB}^{(2)}$ in ~1 ms (pH 7.5); the slow phase is about 2000-fold slower. Biphasic proton uptake kinetics in EQ(L212) RCs have been reported previously in preliminary publications by us (Paddock et al., 1989; Feher et al., 1990; McPherson et al., 1990) and by Takahashi and Wraight (1992). However, these results were obtained in the presence of excess neutral quinone which replaces Q_BH_2 in the Q_B pocket (see Figure 1). As discussed below, a knowledge of the stoichiometry of proton uptake by bound doubly reduced Q_B is important in interpreting the proton uptake kinetics; consequently, we maximized the bound fraction by omitting excess neutral quinone to eliminate the quinol/quinone exchange. In both native and EQ(L212) mutant RCs, the steady-state stoichiometry of proton uptake at pH ≤7.5 was found to be 2.0 protons per Q_B^{2-} ($H^+/2$ e^-) as expected for the formation of Q_BH_2. At pH >7.5, a decrease in proton uptake was observed and was attributed to a pK_a of ~8.5 for the carbonyl oxygen of Q_B that is hydrogen bonded to His-L190 (McPherson et al., 1993a; see also the section on free energy changes).

The kinetics of proton uptake were analyzed using the model shown in Figure 1. The first proton $H^+(1)$ is thought to bind to the oxygen of Q_B that is hydrogen bonded to Ser-L223 (Paddock et al., 1990); its binding is necessary for the electron transfer $k_{AB}^{(2)}$. The uptake of the second proton $H^+(2)$ to the oxygen of Q_B that is hydrogen bonded to His-L190 is thought to occur after electron transfer (Paddock et al., 1990) with a pK_a of ~8.5 [see McPherson et al. (1993a) and below]. We shall discuss this model in terms of the proton uptake by the EQ(L212) RCs starting with the first proton $H^+(1)$.

The hypothesis that the uptake of the first proton $H^+(1)$ is necessary for electron transfer $k_{AB}^{(2)}$ (Paddock et al., 1990) requires that at least one proton be taken up rapidly, i.e., concomitant with the electron transfer. This condition is satisfied in the EQ(L212) mutant RCs, since the stoichiometry of the rapid proton uptake is between 1.1 and 1.4 $H^+/2e^-$, depending on pH (see Table 1). The rapid proton uptake in excess of 1.0 $H^+/2e^-$ is attributed to amino acid residues whose pK_a values are shifted due to interactions with the negative charge of $(Q_BH)^-$. At pH 7.5 and 8.5, this excess proton uptake is within experimental error the same as the proton uptake due to residues that interact with Q_B^- (see Table 1).

We now turn to the second proton $H^+(2)$. The slow phase of the proton uptake by EQ(L212) RCs is attributed to $H^+(2)$ as suggested by the UV difference spectrum (see below). We shall discuss the observed uptake of $H^+(2)$ in terms of the following scheme:

$$Q_A(Q_BH)^- + H^+(2) \underset{k^{off}_{H^+(2)}}{\overset{k^{on}_{H^+(2)}}{\rightleftarrows}} Q_AQ_BH_2 \underset{k^{on}_{Q_BH_2}}{\overset{k^{off}_{Q_BH_2}}{\rightleftarrows}} Q_A + QH_2 \quad (8)$$

Binding of neutral quinone after release of Q_BH_2 is not shown in eq 8 because excess neutral quinone was omitted in the measurements of proton uptake. The relative values of the on and off rates of Q_BH_2 ($k^{on}_{Q_BH_2}$ and $k^{off}_{Q_BH_2}$) are not known [see, e.g., McPherson et al. (1993a) for a discussion]; consequently, the following two cases must be considered:

$k^{off}_{Q_BH_2} \ll k^{on}_{Q_BH_2}$. In this case Q_BH_2 remains bound in the RC, so the second step of eq 8 can be omitted from the analysis. The decrease (~2000-fold) of the observed rate of proton uptake caused by the mutation corresponds to a decrease of the equilibration rate $[H^+]k^{on}_{H^+(2)} + k^{off}_{H^+(2)}$. At pH 7.5, $[H^+]k^{on}_{H^+(2)}$ is at least 10-fold larger than $k^{off}_{H^+(2)}$ in both the mutant and native RCs, as shown by the steady-state proton uptake stoichiometry for doubly reduced Q_B (Table 1).[4] Therefore, at pH 7.5 the equilibration rate is essentially given by $[H^+]k^{on}_{H^+(2)}$; it follows that $k^{on}_{H^+(2)}$ is reduced ~2000-fold by the mutation. Note that if the observed pK_a of $H^+(2)$ is unchanged by the mutation, as suggested by the similar proton uptake stoichiometries in native and EQ(L212) RCs, then the

ratio $k^{on}_{H^+(2)}/k^{off}_{H^+(2)}$ (i.e., the pK_a) must be unchanged; consequently, $k^{on}_{H^+(2)}$ and $k^{off}_{H^+(2)}$ must both be reduced ~2000-fold.

$k^{off}_{Q_BH_2} \gg k^{on}_{Q_BH_2}$. In this case, the release of Q_BH_2 from the RC must be considered in the analysis. A decrease of the on-rate $k^{on}_{H^+(2)}$ of $H^+(2)$ remains the most likely explanation for the slow proton uptake by the mutant. However, several alternate explanations cannot be strictly ruled out by the experimental results and shall be, therefore, discussed. In these alternate schemes, the uptake of $H^+(2)$ to form Q_BH_2 in the RC is energetically unfavorable, i.e., $k^{off}_{H^+(2)} \gg [H^+]k^{on}_{H^+(2)}$. In this case, the equilibration rate $[H^+]k^{on}_{H^+(2)} + k^{off}_{H^+(2)}$ can be fast in both the native and mutant RCs, but the fraction of Q_BH_2 formed in the RC will be too small to observe. The uptake of $H^+(2)$ will be observed only when the subsequent release of Q_BH_2 drives the equilibria shown in eq 8 to completion. If the release rate $k^{off}_{Q_BH_2}$ of Q_BH_2 is the slowest step in the overall reaction, the *observed* rate of uptake of $H^+(2)$ will be $\chi_{Q_BH_2}k^{off}_{Q_BH_2}$, where $\chi_{Q_BH_2}$ is the mole fraction of Q_BH_2, which is determined by the ratio $[H^+]k^{on}_{H^+(2)}/k^{off}_{H^+(2)}$. Consequently, the observed rate of uptake of $H^+(2)$ could be reduced by the mutation through a reduction of either $k^{off}_{Q_BH_2}$ or $\chi_{Q_BH_2}$. We shall discuss $\chi_{Q_BH_2}$ first. Information about $\chi_{Q_BH_2}$ is provided by the stoichiometry of steady-state proton uptake by doubly reduced Q_B (Table 1). This stoichiometry will depend on the free energy difference between the initial and final states in eq 8, i.e., between $Q_A(Q_BH)^-$ and $Q_A + QH_2$. The similar proton uptake stoichiometries for native and EQ(L212) RCs show that the mutation has essentially no effect on the energy of either state. The mole fraction $\chi_{Q_BH_2}$ depends, however, on the free energy difference between $Q_A(Q_BH)^-$ (which is not changed) and $Q_AQ_BH_2$. Could the mutation change the energy of $Q_AQ_BH_2$? This seems unlikely, since $Q_AQ_BH_2$ is electrically neutral and its energy should not, therefore, be affected by the charge of Glu-L212. Furthermore, the crystal structure of the EQ(L212) RCs (Chirino et al., 1994) indicates no changes (<0.5 Å) that could affect the energy of $Q_AQ_BH_2$. Therefore, a reduction of $\chi_{Q_BH_2}$ is unlikely to have occurred. The second alternate explanation for the slow proton uptake is a reduced off-rate $k^{off}_{Q_BH_2}$ of Q_BH_2. This rate is unlikely to have been changed by the mutation because no structural changes that could hinder the release of Q_BH_2 occurred.

We do not know whether $k^{off}_{Q_BH_2}$ or $k^{on}_{Q_BH_2}$ is larger. However, in either case, the most likely explanation for the slow proton uptake in the mutant is a decrease in the on-rate $k^{on}_{H^+(2)}$ of $H^+(2)$. This implicates Glu-L212 as a component of the proton transfer chain. A determination of $k^{on}_{Q_BH_2}$ and $k^{off}_{Q_BH_2}$ would be helpful to completely rule out the alternative hypotheses.

Effect of Q_A^- on the Rate of Uptake of $H^+(2)$. The reduction of Q_A to Q_A^- in EQ(L212) RCs increases the rate of uptake of $H^+(2)$ (see Figure 3); the increase varies from 4-fold (pH 8.0) to 8-fold (pH 6.0). For an activated proton transfer, i.e., where the proton transfer rate is proportional to $\exp(-\Delta G/kT)$, this corresponds to a decrease of 35 meV (pH 8.0) to 55 meV (pH 6.0) in the activation energy ΔG. Two general explanations can account for this effect: (i) *Electrostatic interaction.* The electrostatic field produced by Q_A^- could lower the energy of protonation of doubly reduced Q_B or an intermediate group. If the protonated group is 15 Å from Q_A^- (the approximate distance between Q_A and Q_B), electrostatic interactions of 35 and 55 meV between the charges of Q_A^- and the group would correspond to observed dielectric constants (using Coulombs law) of 27 and 17, respectively. These are within the range of dielectric constants observed in other proteins (Warshel et al., 1984). Why would the observed interaction vary with pH? The reduction of Q_A to Q_A^- causes an uptake of protons by amino acid residues (McPherson et al., 1988; Maroti & Wraight, 1988b); this proton uptake, which varies with pH, would also affect the electrostatic field at the protonated intermediate group. It is interesting that the loss of a positive charge at Arg-M231 ~15 Å from Q_B in the triple mutant Asp-L213 → Ala, Glu-L212 → Ala, Arg-M231 → Leu of *Rhodobacter capsulatus* also speeds up (quantitation not given) the proton uptake (Hanson et al., 1992a). (ii) *Conformational change.* The formation of Q_A^- is believed to cause a conformational change of the RC structure [see Brzezinski et al. (1992) and references therein]. This could lower the activation energy for proton transfer either by changing the orientation of the hydrogen bonds through which proton transfer occurs or by altering the electrostatic field in the RC [see (i)]; the latter could occur, for instance, by a movement of permanent dipoles of the RC protein.

Proton Uptake by DQ_A^- and $DQ_AQ_B^-$. The proton uptake associated with formation of Q_A^- and Q_B^- is due to amino acid residues whose pK_a values are shifted due to interactions with Q_A^- and Q_B^- (Wraight, 1979; McPherson et al., 1988; Maroti & Wraight, 1988a,b). The proton uptake by DQ_A^- at pH >6.5 (see Table 1) is smaller in EQ(L212) RCs than in native RCs. This shows that a significant fraction of the proton uptake by DQ_A^- is due to Glu-L212. It also suggests that Glu-L212 is at least partially ionized at pH ≥7.5 in RCs in the neutral DQ_AQ_B state, in agreement with the results of kinetic IR and FTIR experiments (Hienerwadel et al., 1992) and electrostatic calculations (Gunner & Honig, 1992; Beroza et al., 1994).[5] The proton uptake by $DQ_AQ_B^-$ is also affected by the mutation. At pH ≤7.5, the proton uptake by $DQ_AQ_B^-$ is essentially the same in EQ(L212) and native RCs, but at pH 8.5 it is smaller in the mutant. This shows that Glu-L212 has a significant contribution to the proton uptake by $DQ_AQ_B^-$ at pH >7.5, in agreement with the conclusions reached from the pH dependence of the charge recombination $D^+Q_AQ_B^- \rightarrow DQ_AQ_B$ (Paddock et al., 1989). The similarity of the proton uptakes by $DQ_AQ_B^-$ at pH 7.5 in EQ(L212) and native RCs is surprising in view of the conclusion reached above that Glu-L212 is partially ionized in the neutral DQ_AQ_B state at pH 7.5, which is expected to result in a proton uptake by Glu-L212 after formation of $DQ_AQ_B^-$. However, because Glu-L212 interacts strongly with several other residues (e.g., Asp-L213 and Asp-L210), the effect on proton uptake due to replacements at the L212 site is not simple to predict. A complete understanding of the role of Glu-L212 in proton uptake by DQ_A^- and $DQ_AQ_B^-$ will require measurements over a larger pH range and theoretical calculations of the effects of interactions with other groups.

UV Difference Spectrum Associated with the Slow Proton Uptake. The slow proton uptake by EQ(L212) mutant RCs

[4] The stoichiometry of proton uptake is consistent with a pK_a of $H^+(2)$ of 8.5, i.e., $pK_{H^+(2)} = -\log(k^{off}_{H^+(2)}/k^{on}_{H^+(2)}) = 8.5$. This corresponds to values of 100 (pH 6.5) and 10 (pH 7.5) for the ratio $[H^+]k^{on}_{H^+(2)}/k^{off}_{H^+(2)}$. However, the rate constants $k^{on}_{H^+(2)}$ and $k^{off}_{H^+(2)}$ are probably not pH independent as assumed in this simple analysis, because the observed rate of uptake of $H^+(2)$ decreases about 3-fold per pH unit, in contrast to the 10-fold per pH unit decrease predicted by $[H^+]k^{on}_{H^+(2)}$ for a pH-independent $k^{on}_{H^+(2)}$. Nevertheless, the condition $[H^+]k^{on}_{H^+(2)}/k^{off}_{H^+(2)} > 10$ holds at pH 6.5 and 7.5 as indicated by the uptake of >1.9 protons by Q_B^{2-}.

[5] Note, however, that the different experiments were done at different temperatures, i.e., 21.5 (proton uptake), 15 (FTIR), and 3 °C (kinetic IR).

could be either due to the protonation of $(Q_BH)^-$ or to the protonation of an internal residue (e.g., His-L190) that rapidly transfers a proton to $(Q_BH)^-$. These two possibilities are illustrated by the upper and lower schemes shown in eq 9:

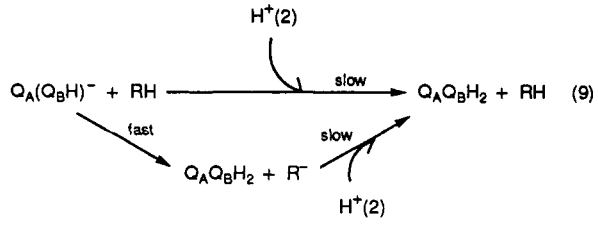

where R represents the putative proton-donating residue. The upper scheme corresponds to the reaction shown in Figure 1. To distinguish between the two schemes, the UV difference spectrum associated with the slow proton uptake by EQ(L212) RCs (see Figure 5) was measured. The difference spectrum observed in EQ(L212) RCs resembles that for the protonation of $(QH)^-$ to QH_2 in 80% ETOH (Morrison et al., 1982) in agreement with the upper scheme of eq 9. The peak at 285 nm corresponds to the formation of Q_BH_2, and the valleys at 310 and <270 nm correspond to the disappearance of $(Q_BH)^-$. The amplitude of the valley at 310 nm is, however, about a factor of 3 smaller in EQ(L212) mutant RCs than in 80% ETOH. Furthermore, the valleys observed at 360 and 400 nm in EQ(L212) RCs are absent in 80% ETOH. The differences between the two spectra may be due to the following: (i) *Overlap of RC absorbance changes with the* $(Q_BH)^-$ *and* Q_BH_2 *absorbances.* The uptake of $H^+(2)$ brings a positive charge into the Q_B site and is expected, therefore, to cause electrochromic band shifts of the RC chromophores (i.e., bacteriopheophytins and bacteriochlorophylls), whose combined absorbances form a peak at 380 nm that is about 60 nm wide at half maximum. These electrochromic shifts could cause the observed valleys at 360 and 400 nm and could partially cancel the valley at 310 nm associated with $(Q_BH)^-$. Electrochromic band shifts of aromatic amino acids (e.g., Trp and Tyr) of the RC protein could contribute at wavelengths below 300 nm. (ii) *Differences between the absorbance of reduced quinone in the RC and in 80% ETOH.* This would, however, be unlikely in view of the good agreement between the absorbance of semiquinone in the RC and in 80% ETOH [see e.g., Morrison et al. (1982). (iii) *Partial rapid protonation of* $(Q_BH)^-$ *to* Q_BH_2 *from an internal residue.* We have assumed in the above discussion that all RCs are in one state, e.g., $Q_A(Q_BH)^-$, before the slow proton uptake. It is possible, however, that the lower scheme in eq 9 prevails but that RH rapidly transfers the proton to $(Q_BH)^-$ in only a fraction of RCs (the fraction would be determined by the difference in pK_as of RH and $Q_AQ_BH_2$).[6] In this case, the observed spectrum would differ from the model spectrum by a scale factor given by the mole fraction of $(Q_BH)^-$. Note that scaling the experimental data in Figure 5 would improve the agreement with the model spectrum at $\lambda < 270$ nm and $295 < \lambda < 330$ nm but would worsen the agreement at $270 < \lambda < 295$ nm.

[6] For the lower scheme shown in eq 9, the ratio of the concentration of the two protonated species is given by a Boltzmann factor:

$$\frac{[Q_BH_2]}{[RH]} = 10^{pK_{Q_BH_2} - pK_{RH}}$$

where these species are out of contact with the outside solvent, i.e., both species cannot be protonated at the same time since only one proton supplied by RH is available. This condition is satisfied in the EQ(L212) mutant for times short compared to that required for the uptake of the second proton (i.e., $t \ll 1$ s).

In conclusion, the UV difference spectrum suggests that $Q_A(Q_BH)^-$ is the state that is present prior to the slow proton uptake, corresponding to the upper scheme of eq 9. A stronger conclusion could perhaps be reached by using a difference spectroscopic technique, e.g., time-resolved FTIR spectroscopy, which is sensitive to the protonation state of reduced quinones (Bauscher et al., 1990).

Additional evidence for the upper scheme shown in eq 9 is provided by an experiment reported by Shinkarev et al. (1993) on chromatophores containing EQ(L212) mutant RCs and the cytochrome bc_1 complex. They found that the light-induced electrogenic reactions of the cytochrome bc_1 complex are absent prior to the slow uptake of the second proton by EQ(L212) RCs. Since the cytochrome bc_1 reactions require quinol that is supplied by release of Q_BH_2 from the RC, Shinkarev et al. concluded that Q_BH_2 is formed slowly in the mutant as shown in the upper scheme of eq 9.

Partition Coefficient β. The transient and steady-state values of the partition coefficient β (see Figure 7 and eqs A.1 and A.2 in the appendix) provide information on the contribution of the two protons $H^+(1)$ and $H^+(2)$ to the driving force for the forward electron transfer. Since the mutation Glu-L212 → Gln has essentially no effect on the stoichiometry of steady-state proton uptake by Q_B^{2-} (see Table 1), the steady-state values of β (β_{ss} in Figure 7), or the rate $k_{AB}^{(2)}$ of the reaction $Q_A^-Q_B^- + H^+(1) \rightarrow Q_A(Q_BH)^-$ (Paddock et al., 1989; Takahashi & Wraight, 1992), the conclusions reached about the free energy changes associated with the uptake of $H^+(1)$ and $H^+(2)$ by the mutant RCs should also apply to native RCs. The steady-state value of β (β_{ss}) refers to the partitioning between $Q_A^-Q_B^-$ and Q_B^{2-} after the uptakes of both $H^+(1)$ and $H^+(2)$ have come to equilibrium (see eqs A.1 and A.2b). The pH profiles (Figure 7) of β_{ss} in native and EQ(L212) RCs are similar. The transient value of β in EQ(L212) RCs (β_{trans}; see Figure 7b) refers to the partitioning between $Q_A^-Q_B^-$ and Q_B^{2-} after the fast proton uptake and electron transfer $k_{AB}^{(2)}$ but before the slow proton uptake (see eqs A.1 and A.2a in the Appendix); in native RCs, the uptake of $H^+(2)$ is too rapid for a measurement of β_{trans}. At pH <8.5, the uptake of the first proton $H^+(1)$ supplies sufficient driving force for electron transfer to occur in more than 90% of the RCs; i.e., β_{trans} is less than 0.1, but at pH >9.0 the electron transfer and uptake of $H^+(1)$ become energetically unfavorable. The uptake of the second proton $H^+(2)$ supplies only a minor amount of additional driving force for the electron transfer at pH >8.5, as shown by the small difference between β_{trans} and β_{ss}. The driving forces are quantified in the next section.

Free Energy Changes Associated with Electron and Proton Transfer. We used the scheme shown in eq 10 to model the free energy changes associated with the uptake of $H^+(1)$ and $H^+(2)$ in EQ(L212) RCs:

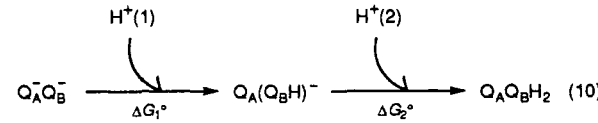

The free energies ΔG_1° and ΔG_2° (Table 2) were calculated from β_{trans} and β_{ss} (defined in eq A.1 in the appendix) using the following relations (derived in the appendix):

$$\Delta G_1^\circ = -kT \ln\left\{\frac{1-\beta_{trans}}{\beta_{trans}}\right\} \quad (11a)$$

$$\Delta G_2^\circ = -kT \ln\left\{\frac{1-\beta_{ss}}{\beta_{ss}}\frac{\beta_{trans}}{1-\beta_{trans}} - 1\right\} \quad (11b)$$

where k is Boltzmann's constant and T the absolute tem-

Table 2: Free Energy Changes Associated with Electron and Proton Transfer $Q_A^-Q_B^- + 2H^+ \rightarrow Q_AQ_BH_2$ in EQ (L212) RCs[a]

pH	ΔG_1° (meV)	ΔG_2° (meV)	$pK_{H^+(2)}$
7.5	−70 ± 20	ND	ND
8.0	−70 ± 20	ND	ND
8.5	−34 ± 6	ND	ND
9.0	−3 ± 6	≥0 ± 20	≤ 9.0 ± 0.3
9.5	+25 ± 14	≥+28 ± 20	≤9.0 ± 0.3

[a] ΔG_1° is free energy difference between $Q_A^-Q_B^-$ and $Q_A(Q_BH)^-$ (see eq 10) and was determined from the transient value of the partition coefficient β (Figure 7b) using eq 11a. ΔG_2° is free energy difference between $Q_A(Q_BH)^-$ and $Q_AQ_BH_2$ and was determined from the transient and steady-state values of the partition coefficient β (Figure 7b) using eq 11b. The values determined for ΔG_2° may include a small negative contribution due to exchange of quinone with quinol in a fraction (0.2) of RCs and are, therefore, given as lower limits; ΔG_2° was not determined (ND) at pH values where the experimental uncertainty in the lower limit was >20 meV. $pK_{H^+(2)}$ is the pK_a associated with the second proton $H^+(2)$ and was determined from ΔG_2° using eq 13.

perature. Only a lower limit is given for ΔG_2° because a small fraction (0.20; see Materials and Methods) of RCs contained nonspecifically bound neutral quinone, which may have exchanged with Q_BH_2, and, therefore, partially driven the slow proton uptake. Furthermore, Q_BH_2 may be released from the RC even in the absence of extra neutral quinone [see, e.g., the discussion by McPherson et al. (1993a)], which would also drive the slow proton uptake.

The free energy ΔG_1° between $Q_A^-Q_B^-$ and $Q_A(Q_BH)^-$ (see eq 10 and Table 2) has a linear pH dependence at pH 8.0–9.5 with a slope of 63 ± 3 meV/pH. This pH dependence is caused by the uptake of $H^+(1)$ and can be modeled in the linear range by the following simple expression:[7]

$$\Delta G_1^\circ = \Delta G_{ET}^\circ + 2.3kT[\mathrm{pH} - pK_{H^+(1)}(Q_B^{2-})] \quad (12)$$

where $pK_{H^+(1)}(Q_B^{2-})$ is the pK_a of $H^+(1)$ for the state Q_B^{2-} and ΔG_{ET}° is the (pH-independent) free energy change for the electron transfer $Q_A^-Q_B^- \rightarrow Q_AQ_B^{2-}$ without protonation. Equation 12 is valid for $pK_{H^+(1)}(Q_A^-Q_B^-) \ll \mathrm{pH} \ll pK_{H^+(1)}(Q_B^{2-})$, where $pK_{H^+(1)}(Q_A^-Q_B^-)$ is the pK_a of $H^+(1)$ for the state $Q_A^-Q_B^-$. Equation 12 predicts a slope of $2.3kT$/pH (i.e., 60 meV/pH at 300 K) in agreement with the observed value. Outside the range $pK_{H^+(1)}(Q_A^-Q_B^-) \ll \mathrm{pH} \ll pK_{H^+(1)}(Q_B^{2-})$, ΔG_1° is expected to be independent of pH [see, e.g., Kleinfeld et al. (1985), McPherson et al. (1988), and Takahashi and Wraight (1992)]; the observed linear pH dependence of ΔG_1° between pH 8.0 and 9.5 suggests the limits $pK_{H^+(1)}(Q_A^-Q_B^-) < 8$ and $pK_{H^+(1)}(Q_B^{2-}) > 10$. Takahashi and Wraight (1992) have reached similar conclusions.

A knowledge of the values of ΔG_{ET}° and $pK_{H^+(1)}$ is important for an understanding of the mechanism of transfer of the second electron to Q_B^- [see e.g., Okamura and Feher (1992) and Paddock et al. (1993)]. A question that has not yet been answered is whether the second electron transfer precedes or follows the uptake of $H^+(1)$ [for recent discussions, see, e.g., Maroti and Wraight (1990), Okamura and Feher (1992), and Paddock et al. (1993)], i.e., whether the activated intermediate state in the reaction of Figure 1 and eq 10 involving $H^+(1)$ and $k_{AB}^{(2)}$ is $Q_AQ_B^{2-}$ (unprotonated) or $Q_A^-(Q_BH)$. Since the dominant intermediate state will be the one of lower energy relative to $Q_A^-Q_B^-$, determination of the energy ΔG_{ET}° between $Q_A^-Q_B^-$ and $Q_AQ_B^{2-}$ and the energy $\Delta G_{H^+}^\circ$ between $Q_A^-Q_B^-$ and $Q_A^-(Q_BH)$ should help answer this question. The energy ΔG_{ET}° could be determined by using eq 12 and the values of ΔG_1° in Table 2 if $pK_{H^+(1)}(Q_B^{2-})$ were known. It may be possible to measure $pK_{H^+(1)}(Q_B^{2-})$ by spectrophotometric pH titration of doubly reduced Q_B (Morrison et al., 1982). The energy $\Delta G_{H^+}^\circ$ between $Q_A^-Q_B^-$ and $Q_A^-(Q_BH)$ is determined by the difference between the pH and the pK_a of $Q_A^-Q_B^-$ [$pK_{H^+(1)}(Q_A^-Q_B^-)$], which can in principle be measured spectroscopically at 450 nm. Although neither $pK_{H^+(1)}(Q_B^{2-})$ nor $pK_{H^+(1)}(Q_A^-Q_B^-)$ has yet been determined, we have obtained rough estimates of these values using a simplified analysis. Regarding the pK_a for the state $Q_AQ_B^{2-}$, the value of $pK_{H^+(1)}(Q_B^{2-})$ can be estimated to be 10.5, i.e., 1.5 units larger than the pK_a of the second proton $H^+(2)$ (discussed below). This is based on the observation that, for a variety of benzohydroquinones in water, the pK_a of $H^+(1)$ is 1.5 units larger than that of $H^+(2)$ (Morrison et al., 1982). For $pK_{H^+(1)}(Q_B^{2-}) = 10.5$, eq 12 predicts that the free energy ΔG_{ET}° between $Q_A^-Q_B^-$ and $Q_AQ_B^{2-}$ is +90 meV.[8] Regarding the pK_a for the state $Q_A^-Q_B^-$, the value of $pK_{H^+(1)}(Q_A^-Q_B^-)$ might be less than 4.0 based on the fact that protonated semiquinone has never been observed in the RC even at low pH [down to pH 5; see, e.g., Okamura and Feher (1992)]. For $pK_{H^+(1)}(Q_A^-Q_B^-) = 4.0$, the free energy $\Delta G_{H^+}^\circ$ between $Q_A^-Q_B^-$ and $Q_A(Q_BH)$ is +240 meV at pH 8.0. If the rough estimates of +90 meV for ΔG_{ET}° and +240 meV for $\Delta G_{H^+}^\circ$ at pH 8.0 are correct, then $Q_AQ_B^{2-}$ may provide an intermediate state between $Q_A^-Q_B^-$ and $Q_A(Q_BH)^-$. An accurate measurement of $pK_{H^+(1)}(Q_A^-Q_B^-)$ and $pK_{H^+(1)}(Q_B^{2-})$ should make a definitive determination of the intermediate state possible.

We now turn to the free energy ΔG_2° between the states $Q_A(Q_BH)^-$ and $Q_AQ_BH_2$ (see eq 10). At pH ≥ 9 ΔG_2° is ≥0 (see Table 2), indicating that the uptake of the second proton $H^+(2)$ is energetically unfavorable at pH ≥9. This explains why there is only a minor difference between β_{trans} and β_{ss} at pH >8.5 (see figure 7b). A pK_a for $H^+(2)$ can be calculated directly from the free energy change as follows:

$$pK_{H^+(2)} = \mathrm{pH} - \frac{\Delta G_2^\circ}{2.3kT} \quad (13)$$

The pK_a thus determined (see Table 2) is less than 9.0. This value is in agreement with the apparent pK_a of 8.5 observed for the steady-state proton uptake by Q_B^{2-} in native and EQ(L212) RCs. According to the model shown in eq 10, this pK_a corresponds to the protonation of the carbonyl oxygen of Q_B, presumably the one near Glu–L212 and hydrogen bonded to His-L190 (McPherson et al., 1993a).[9] The value of $pK_{H^+(2)}$ is significantly less than the value of ~13 determined for ubihydroquinone in 80% ETOH (Morrison et al., 1982). However, pK_as in the reaction center can be significantly different than those in solution, due, e.g., to electrostatic interactions between protonatable groups. A detailed dis-

[7] See, e.g., Kleinfeld et al. (1985) or McPherson et al. (1988) for a general discussion of the effect of proton uptake on the free energy change associated with an electron transfer reaction.

[8] Paddock et al. (1993) have estimated a limit $\Delta G_{ET}^0 \geq +220$ meV in native RCs based on a comparison of cytochrome c photooxidation and electron transfer $k_{AB}^{(2)}$. If that number is used in eq 12, then $pK_{H^+(1)}(Q_B^{2-})$ would be ≥13 rather than the assumed 10.5 that gave the value of +90 meV for ΔG_{ET}^0. In this case the formation of $Q_AQ_B^{2-}$ is less likely.

[9] The model in eq 10 is based on the interpretation of the UV difference spectrum, which suggests that the slow uptake of $H^+(2)$ corresponds to the protonation of the carbonyl oxygen of Q_B. Should this interpretation prove to be incorrect, i.e., if the slow uptake of $H^+(2)$ is the protonation of a residue, the pK_a of ~8.5 and the free energy ΔG_2° would apply to the protonation of the residue rather than the carbonyl oxygen. A discussion of which residues might be involved in this case is given by McPherson et al. (1993a).

cussion of the possible reasons for a lower pK_a is given by McPherson et al. (1993a).

The observed free energy ΔG°_{obs} between $Q_A^-Q_B^-$ and $Q_AQ_B^{2-}$ (protonation omitted for simplicity) in native RCs has been discussed by Kleinfeld et al. (1985). Their data apply to an admixture of all the protonated states shown in eq 10. The pH dependence of ΔG°_{obs} between pH 8 and 11 with an apparent $pK_a > 10.7$ was attributed to the second proton $H^+(2)$. However, the above results suggest that the pK_a of $H^+(2)$ is significantly lower in both native and EQ(L212) RCs and that the pH dependence of ΔG°_{obs} at pH >9 is, therefore, dominated by the uptake of $H^+(1)$. Therefore, the limit of 10.7 applies to $pK_{H^+(1)}$.

Role of Glu-L212 in Proton Transfer. The proton uptake kinetics in EQ(L212) RCs indicate that Glu-L212 is part of the proton transfer pathway of the second proton $H^+(2)$ in native RCs from *Rb. sphaeroides*. Glu-L212 probably serves a similar role in other species of bacteria in which it is conserved [see, e.g., Ovchinnikov et al. (1988)], e.g., *Rb. capsulatus*. Although Glu-L212 provides the best pathway in native RCs, other pathways are possible. For example, in *Rb. capsulatus*, although Glu-L212 is involved in proton transfer, alternate pathways without Glu-L212 can also be active (Hanson et al., 1992a,b; Schiffer et al., 1992).

One question about the role of Glu-L212 is whether it transfers a proton *directly* to reduced Q_B or *indirectly* through either another residue or a bound water molecule (Paddock et al., 1990; Beroza et al., 1992). An analysis of the RC structure (Beroza et al., 1992) suggests that, in the case of an indirect transfer, His-L190 (hydrogen bonded to the carbonyl oxygen of Q_B) is essentially the only possibility for an intervening group between Glu-L212 and Q_B. The carboxyl oxygen of Glu-L212 is 5.1 Å from the carbonyl oxygen of Q_B and 5.9 Å from the nitrogen of the imidazol ring of His-L190 (Beroza et al., 1992). Consequently, proton transfer from Glu-L212 to either one of these groups would require movement of either Q_B or of the amino acid residue to reduce the distance to within that of a hydrogen bond (~3 Å). It was previously suggested that internal proton transfer from His-L190 to reduce Q_B (followed by proton transfer from Glu-L212 to His-L190) may be necessary for the second electron transfer $k_{AB}^{(2)}$ (Paddock et al., 1990). However, the UV difference spectrum discussed in this work suggests that this is not the case. Further evidence against the involvement of His-L190 is provided by results from the replacement of His-L190 with Gln. This mutation had very little effect on the overall rate of the RC photocycle (Williams et al., unpublished results) indicating that His-L190 is not crucial for proton transfer. Therefore, the experimental evidence and the analysis of the crystal structure (Beroza et al., 1992) suggest that Glu-L212 transfers a proton directly to the oxygen of doubly reduced Q_B following a reduction in the distance between Q_B and Glu-L212.

From where does Glu-L212 obtain the proton? Inspection of the crystal structure of the RC indicates several possible pathways leading to Glu-L212 (Beroza et al., 1992), including one involving Asp-L213 and bound water molecules between Asp-L213 and Glu-L212. Experimental evidence (McPherson et al., 1991; Okamura & Feher, 1992) supports the involvement of Asp-L213 in the uptake of $H^+(2)$. Higher resolution X-ray data of RC crystals in which bound water molecules are resolved (for oxidized and reduced Q_B) should provide additional information on the roles of the residues and bound water in the proton transfer to and from Glu-L212.

ACKNOWLEDGMENT

We thank Ed Abresch for purifying the RCs.

APPENDIX

Equations 11a and 11b, used to determine the free energy changes ΔG_1° and ΔG_2° (defined in eq 10) from the measured values of the partition coefficient β, are derived below. The transient (β_{trans}) and steady-state (β_{ss}) β refers to the equilibrium between $Q_A^-Q_B^-$ and doubly reduced Q_B before and after the slow uptake of $H^+(2)$ as shown in eq A.1:

$$Q_A^-Q_B^- \underset{}{\overset{H^+(1)}{\rightleftharpoons}} Q_A(Q_BH)^- \overset{H^+(2)}{\rightleftharpoons} Q_AQ_BH_2 \qquad \beta_{trans},\ \beta_{ss} \qquad \text{(A.1)}$$

β_{trans} and β_{ss} are given by the following:

$$\beta_{trans} = \frac{[Q_A^-Q_B^-]}{[Q_A^-Q_B^-] + [Q_A(Q_BH)^-]} = \frac{1}{1 + \dfrac{[Q_A(Q_BH)^-]}{[Q_A^-Q_B^-]}} \qquad \text{(A.2a)}$$

$$\beta_{ss} = \frac{[Q_A^-Q_B^-]}{[Q_A^-Q_B^-] + [Q_A(Q_BH)^-] + [Q_AQ_BH_2]} = \frac{1}{1 + \dfrac{[Q_A(Q_BH)^-]}{[Q_A^-Q_B^-]} + \dfrac{[Q_AQ_BH_2]}{[Q_A^-Q_B^-]}} \qquad \text{(A.2b)}$$

The ratios of concentrations shown in eqs A.2a,b are given in terms of ΔG_1° and ΔG_2° by Boltzmann factors:

$$\frac{[Q_A(Q_BH)^-]}{[Q_A^-Q_B^-]} = e^{-\Delta G_1^\circ/kT} \qquad \text{(A.3a)}$$

$$\frac{[Q_AQ_BH_2]}{[Q_A^-Q_B^-]} = e^{-(\Delta G_1^\circ + \Delta G_2^\circ)/kT} \qquad \text{(A.3b)}$$

Substitution of eqs A.3 into eqs A.2 and algebraic manipulation leads to eqs 11a,b.

REFERENCES

Allen, J. P., Feher, G., Yeates, T. O., Komiya, H., & Rees, D. C. (1988) *Proc. Natl. Acad. Sci. U.S.A. 85*, 8487–8491.

Bauscher, M., Nabedryk, E., Bagley, K., Breton, J., & Mantele, W. (1990) *FEBS Lett. 261*, 191–195.

Beroza, P., Fredkin, D. R., Okamura, M. Y., & Feher, G. (1992) in *The Photosynthetic Bacterial Reaction Center II* (Breton, J., & Vermeglio, A., Eds.) pp 363–374, Plenum Press, New York.

Beroza, P., Fredkin, D. R., Okamura, M. Y., & Feher, G. (1994) *Biophys. J. (Abstr.)* (in press).

Brzezinski, P., Okamura, M. Y., & Feher, G. (1992) in *The Photosynthetic Bacterial Reaction Center II* (Breton, J., & Vermeglio, A., Eds.) pp 321–330, Plenum Press, New York.

Chirino, A. J., Lous, E. J., Huber, M., Allen, J. P., Schenck, C. C., Paddock, M. L., Feher, G., & Rees, D. C. (1994) *Biochemistry* (submitted).

Cramer, W. A., & Knaff, D. B. (1990) *Energy Transduction in Biological Membranes*, Springer-Verlag, New York.

Dutton, P. L. (1986) in *Encylcopedia of Plant Physiology Vol. 19: Photosynthesis III* (Staehelin, L. A., & Arntzen, C. J., Eds.) pp 197–237, Springer, New York.

Feher, G., Allen, J. P., Okamura, M. Y., & Rees, D. C. (1989) *Nature 339*, 111–116.

Feher, G., McPherson, P. H., Paddock, M. L., Rongey, S., Schonfeld, M., & Okamura, M. Y., (1990) in *Current Research in Photosynthesis* (Baltscheffsky, M., Ed.) Vol. I, pp I.1.39–46, Kluwer, Dordrecht, The Netherlands.

Gunner, M. R., & Honig, B. (1992) in *The Photosynthetic Bacterial Reaction Center II* (Breton, J., & Vermeglio, A. Eds.) pp 403–410, Plenum Press, New York.

Hanson, D. K., Baciou, L., Tiede, D. M., Nance, S. L., Schiffer, M., & Sebban, P. (1992a) *Biochim. Biophys. Acta 1102*, 260–265.

Hanson, D. K., Nance, S. L., & Schiffer, M. (1992b) *Photosynth. Res. 32*, 147–153.

Hienerwadel, R., Nabedryk, E., Paddock, M. L., Rongey, S. H., Okamura, M. Y., Mantele, W., & Breton, J. (1992) in *Research in Photosynthesis* (Murata, N., Ed.) Vol. I, pp I.3.437–440, Kluwer, Dordrecht, The Netherlands.

Kirmaier, C., & Holten, D. (1987) *Photosynth. Res. 13*, 225–260.

Kleinfeld, D., Okamura, M. Y., & Feher, G. (1984) *Biochim. Biophys. Acta 766*, 126–140.

Kleinfeld, D., Okamura, M. Y., & Feher, G. (1985) *Biochim. Biophys. Acta 809*, 291–310.

Maroti, P., & Wraight, C. A. (1988a) *Biochim. Biophys. Acta 934*, 314–328.

Maroti, P., & Wraight, C. A. (1988b) *Biochim. Biophys. Acta 934*, 329–347.

Maroti, P., & Wraight, C. A. (1990) in *Current Research in Photosynthesis* (Baltscheffsky, M., Ed.) Vol. I, pp 165–168, Kluwer, Dordrecht, The Netherlands.

McPherson, P. H., Okamura, M. Y., & Feher, G. (1988) *Biochim. Biophys. Acta 934*, 348–368.

McPherson, P. H., Schönfeld, M., Paddock, M. L., Feher, G., & Okamura, M. Y. (1990) *Biophys. J. (Abstr) 57*, 404a.

McPherson, P. H., Rongey, S. H., Paddock, M. L., Feher, G., & Okamura, M. Y., (1991) *Biophys. J. (Abstr) 59*, 142a.

McPherson, P. H., Okamura, M. Y., Feher, G. (1993a) *Biochim. Biophys. Acta 1144*, 309–324.

McPherson, P. H., Paddock, M. L., Okamura, M. Y., & Feher, G. (1993b) *Biophys. J. (Abstr) 64*, A18.

Morrison, L. E., Schelhorn, J. E., Cotton, T. M., Bering, C. L., & Loach, P. A. (1982) in *Function of Quinones in Energy-Conserving Systems* (Trumpower, B. L., Ed.) pp 35–58, Academic Press, New York.

Nicholls, D. G. (1982) *Bioenergetics: an Introduction to the Chemiosmotic Theory*, Academic Press, New York.

Okamura, M. Y., & Feher, G. (1992) *Annu. Rev. Biochem. 61*, 861–896.

Okamura, M. Y., Isaacson, R. A., & Feher, G. (1975) *Proc. Natl. Acad. Sci. U.S.A. 72*, 3491–3495.

Okamura, M. Y., Debus, R. J., Kleinfeld, D., & Feher, G. (1982) in *Function of Quinones in Energy-Conserving Systems* (Trumpower, B. L., Ed.) pp 299–317, Academic Press, New York.

Ovchinnikov, Y. A., Abdulaev, N. G., Zolotarev, A. S., Shmukler, B. E., Zargarov, A. A., Kutuzov, M. A., Telezhinskaya, I. N., & Levina, N. B. (1988) *FEBS Lett. 231*, 237–242.

Paddock, M. L., Rongey, S. H., Abresch, E. C., Feher, G., & Okamura, M. Y. (1988) *Photosynth. Res. 17*, 75–96.

Paddock, M. L., Rongey, S. H., Feher, G., & Okamura, M. Y. (1989) *Proc. Natl. Acad. Sci. U.S.A. 86*, 6602–6606.

Paddock, M. L., McPherson, P. H., Feher, G., & Okamura, M. Y. (1990) *Proc. Natl. Acad. Sci. U.S.A. 87*, 6803–6807.

Paddock, M. L., Rongey, S. H., McPherson, P. H., Juth, A., Feher, G., & Okamura, M. Y. (1994) *Biochemistry* (in press).

Parson, W. W. (1987) in *Photosynthesis* (Amesz, J., Ed.) pp 43–61, Elsevier, New York.

Schiffer, M., Chan, C.-K., Chang, C.-H., Dimagno, T. J., Fleming, G. R., Nance, S., Norris, J., Snyder, S., Thurnauer, M., Tiede, D. M., & Hanson, D. K. (1992) in *The Photosynthetic Bacterial Reaction Center II* (Breton, J., & Vermeglio, A., Eds.) pp 351–361, Plenum Press, New York.

Shinkarev, V. P., Takahashi, E., & Wraight, C. A. (1993) *Biochim. Biophys. Acta 1142*, 214–216.

Takahashi, E., & Wraight, C. A. (1990) *Biochim. Biophys. Acta 1020*, 107–111.

Takahashi, E., & Wraight, C. A. (1992) *Biochemistry 31*, 855–866.

Takahashi, E., & Wraight, C. A. (1993) in *Advances in Molecular and Cell Biology* (Barber, J., Ed.) JAI Press, Greenwich, CT.

Van Gelder, B. F., & Slater, E. C. (1962) *Biochim. Biophys. Acta 58*, 593–595.

Warshel, A., Russell, S. T., & Churg, A. K. (1984) *Proc. Natl. Acad. Sci. U.S.A. 81*, 4785–4789.

Wraight, C. A. (1979) *Biochim. Biophys. Acta 548*, 309–327.

Wraight, C. A. (1982) in *Function of Quinones in Energy-Conserving Systems* (Trumpower, B. L., Ed.) p 181–197, Academic Press, New York.